TOMSK POLYTECHNIC UNIVERSITY ТОМСКИЙ ПОЛИТЕХНИЧЕСКИЙ УНИВЕРСИТЕТ

Министерство науки и высшего образования Российской Федерации
федеральное государственное автономное
образовательное учреждение высшего образования
«Национальный исследовательский Томский политехнический университет» (ТПУ)

Инженерная школа ядерных технологий
Направление подготовки 14.04.02 Ядерные физика и технологии
Отделение ядерно-топливного цикла

МАГИСТЕРСКАЯ ДИССЕРТАЦИЯ

Тема работы
Физико-математические основы лучевой диагностики и терапии

УДК : 615.949:51:53

Студент

Группа	ФИО	Подпись	Дата
0АМ0М	Асиама Самуэль Йо		

Руководитель ВКР

Должность	ФИО	Ученая степень, звание	Подпись	Дата
профессор ИШХБМТ ТПУ	Бразовский К.С.	д.т.н.		

КОНСУЛЬТАНТЫ ПО РАЗДЕЛАМ:

По разделу «Финансовый менеджмент, ресурсоэффективность и ресурсосбережение»

Должность	ФИО	Ученая степень, звание	Подпись	Дата
Доцент ОСГН ШИП	Спицына Л.Ю.	к.э.н.		

По разделу «Социальная ответственность»

Должность	ФИО	Ученая степень, звание	Подпись	Дата
Доцент ОЯТЦ ИЯТШ	Передерин Ю.В.	к.т.н		

ДОПУСТИТЬ К ЗАЩИТЕ:

Руководитель ООП	ФИО	Ученая степень, звание	Подпись	Дата
Ядерные реакторы энергетические установки/Ядерная медицин	Верхотурова В.В.	к.и.н.		

Томск – 2022 г.

TOMSK POLYTECHNIC UNIVERSITY ТОМСКИЙ ПОЛИТЕХНИЧЕСКИЙ УНИВЕРСИТЕТ

Министерство науки и высшего образования Российской Федерации
федеральное государственное автономное
образовательное учреждение высшего образования
«Национальный исследовательский Томский политехнический университет» (ТПУ)

School of Nuclear Science & Engineering
Field of training: 14.04.02 Nuclear Science and Technology
Specialization: Nuclear Power Engineering / Nuclear medicine
Nuclear Fuel Cycle Division

MASTER THESIS

Topic of research work
Physical and mathematical foundations of radiation diagnostics and therapy

UDC: 615.949:51:53

Student

Group	Full name	Signature	Date
0AM0M	Asiamah Samuel Yaw		

Scientific supervisor

Position	Full name	Academic degree, academic rank	Signature	Date
Professor (ISHKHBMT)	Konstantin Brazovsky	Ph.D.		

ADVISERS:

Section “Financial Management, Resource Efficiency and Resource Saving”

Position	Full name	Academic degree, academic rank	Signature	Date
Associate Professor	Luibov Y. Spicyna	PhD		

Section “Social Responsibility”

Position	Full name	Academic degree, academic rank	Signature	Date
Associate Professor	Yuriy V. Perederin	PhD		

ADMITTED TO DEFENSE:

Programme Director	Full name	Academic degree, academic rank	Signature	Date
Nuclear Power Engineering / Nuclear medicine	Vera V. Verkhoturova	PhD		

Tomsk – 2022

LEARNING OUTCOMES

Competence code	Competence name
Universal competences	
UC(U)-1	Ability to make critical analysis of problem-based situations using the systems analysis approach, and generate decisions and action plans.
UC(U)-2	Ability to run a project at all life-cycle stages.
UC(U)-3	Ability to organize and lead the teamwork and generate a team strategy to achieve the target goal.
UC(U)-4	Ability to use modern communication technologies to realize academic and professional interaction.
UC(U)-5	Ability to analyze and account for cultural diversity in the process of intercultural interaction.
UC(U)-6	Ability to set and pursue individual and professional activity priorities and ways to modify professional activity based on the self-esteem.
General professional competences	
GPC(U)-1	Ability to formulate goals and objectives of the research study, select assessment criteria, identify priorities for solving problems.
GPC(U)-2	Ability to apply modern research methods, evaluate and present the results of the performed research.
GPC(U)-3	Ability to present research outcomes in the form of articles, reports, scientific reports and presentations using computer layout systems and office software packages.
Professional competences	
PC(U)-1	Ability to maintain medical and technical documentation related to medico-physical aspects of radiation therapy, interventional radiology and radionuclide diagnostics and therapy.
PC(U)-2	Ability to ensure radiation safety of personnel, public, and the environment, to carry out monitoring of radiation exposure levels of patients, personnel, public, and the environment.
PC(U)-3	Ability to operate and maintain equipment and tools applied for the medical use of radiation.

PC(U)-4	Ability to manage the quality of physical and technical aspects within radiation therapy, diagnostics, interventional radiology and radionuclide diagnostics and therapy departments in accordance with the specific equipment requirements, regulatory requirements and staffing of a medical organization.
PC(U)-5	Ability to conduct and organize dosimetry planning, clinical dosimetry, quality assurance procedures for radiotherapy, interventional radiology, and radionuclide diagnostics and therapy.
PC(U)-6	Ability to apply knowledge of natural sciences, fundamental laws in the field of nuclear physics and technology, clinical and radiation standards, hygienic measures in nuclear medicine, which is sufficient to study issues associated with medical physics using modern equipment and information technology relying on the latest Russian and international experience.
PC(U)-7	Ability to develop reference books, tables and software containing data for clinical use in dosimetric planning of radiation therapy, radionuclide diagnostics and therapy.
PC(U)-8	Ability to take part in the design and physical and technical equipment development for radiation therapy, diagnostics, interventional radiology and radionuclide diagnostics and therapy, and radiation safety divisions.
PC(U)-9	Ability to conduct training sessions and develop instructional materials for the training courses within the cycle of professional training programs (bachelor degree programs).

TOMSK POLYTECHNIC UNIVERSITY ТОМСКИЙ ПОЛИТЕХНИЧЕСКИЙ УНИВЕРСИТЕТ

Министерство науки и высшего образования Российской Федерации
федеральное государственное автономное
образовательное учреждение высшего образования
«Национальный исследовательский Томский политехнический университет» (ТПУ)

School of Nuclear Science & Engineering
Field of training: 14.04.02 Nuclear Science and Technology
Specialization: Nuclear Power Engineering / Nuclear medicine/ Nuclear Fuel Cycle Division

APPROVED BY:
Program Director
_____ Verkhoturova V.V.
«____» _____ 2022

ASSIGNMENT
for the Graduation Thesis completion

In the form:

Master Thesis

For a student:

Group	Full name
0AM0M	Asiamah Samuel Yaw

Topic of research work:

Physical and mathematical foundations of radiation diagnostics and therapy	
Approved by the order of the Director of School of Nuclear Science & Engineering (date, number):	№ 32-6/c dated February 1, 2022

Deadline for completion of Master Thesis:	06.06.2022

TERMS OF REFERENCE:

Initial date for research work: *(the name of the object of research or design; performance or load; mode of operation (continuous, periodic, cyclic, etc.); type of raw material or material of the product; requirements for the product, product or process; special requirements to the features of the operation of the object or product in terms of operational*	Papers and journals on the applications of mathematics and nuclear physics in medical imaging. Object of research-the study of algorithm of 1D, 2D tomographic analysis. Type of the algorithm – Filtered back-projection algorithm and Radon Transform algorithm.

safety, environmental impact, energy costs; economic analysis, etc.)	
List of the issues to be investigated, designed and developed *(analytical review of literary sources with the purpose to study global scientific and technological achievements in the target field, formulation of the research purpose, design, construction, determination of the procedure for research, design, and construction, discussion of the research work results, formulation of additional sections to be developed; conclusions).*	**Theoretical aspect** 1. History and general understanding of radiation therapy. 2. Contributions of physics and mathematics in medical imaging and radiation therapy.. 3. Types of radiation used in radiation therapy. 4. Imaging techniques and process of image project and reconstructions. **Practical aspect** 1. MATLAB and WOLFRAM programming Language training in image projection and reconstructio
List of graphic material *(with an exact indication of mandatory drawings)*	Block scheme of the developed algorithm

Advisors to the sections of the Master Thesis
(with indication of sections)

Section	Advisor
Literature review	Konstantin Brazovsky Ph.D. Professor (ISHKHBMT)
Theoretical aspect of the reconstruction	Konstantin Brazovsky Ph.D. Professor (ISHKHBMT)
Practical aspect of the reconstruction	Bogdanov A.Viktorovich Senior Lecturer (OMI, ShBIP
Social responsibility	Yuriy V. Perederin, PhD
Financial management	Luibov Y. Spicyna, PhD

Date of issuance of the assignment for Master Thesis completion according to the schedule	

Assignment issued by a scientific supervisor / advisor (if any):

Position	Full name	Academic degree, academic status	Signature	Date
Associate Professor	Konstantin Brazovsky	Ph.D.Professor (ISHKHBMT)		

Assignment accepted for execution by a student:

Group	Full name	Signature	Date
0AM0M	Asiamah Samuel Yaw		

TASK FOR SECTION

«FINANCIAL MANAGEMENT, RESOURCE EFFICIENCY AND RESOURCE SAVING»

For a student:

Group	Full name
0AM0M	Asiamah Samuel Yaw

School	Nuclear Science and Engineering	Department	Nuclear fuel cycle
Degree	Master programme	**Field of training/programme**	14.04.02. Nuclear physics and technology/ Nuclear medicine

Initial data for chapter «FINANCIAL MANAGEMENT, RESOURCE EFFICIENCY AND RESOURCE SAVING»:	
1. *The cost of scientific research resources: material, technical, energy, financial, informational and human*	*Project budget 448123,78 rubles:* *The cost of purchasing equipment – 72 thousand rubles, the cost of a salary for a supervisor – 93 thousand rubles, the cost of a salary for a design engineer – 18 thousand rubles. etc.*
2. *The system of taxation used, tax rates, volumes of payments, discounts and loans*	*According to clause 3 of subclause 16 of Art. 149 of the Tax Code of the Russian Federation, this project is not subject to taxation. Based on Chapter 34 of the Tax Code of the Russian Federation, since 2016, the rate of 30.2% of the wage fund has been used to calculate contributions to extra-budgetary funds.*
Problems to research, calculate and describe:	
1. Project initiation	Project goals and results, project structure, assumptions and limitations, planning, budgeting, etc.
2. Economic model development	Calculation of initial investment, calculation of funds obtained from fuel savings, calculation of cash flows over 20 years
3. Determining the effectiveness of projects	Net Present Value Calculation and Sensitivity Analysis
4. Final decision making	Selecting and evaluating criteria, weighing the criteria and calculating the most appropriate solution
Graphic materials:	
1. «Portrait» of the consumer *2. Competitive power of the project* *3. SWOT matrix* *4. Assessment of the prospects of a new product* *5. Plan of investments. The budget for scientific and technical research*	

Assignment date	

The task was issued by consultant:

Position	Full name	Academic degree, academic rank	Signature	Date
Associate Professor	Spitsyna L. Yu.	Ph.D		

The task was accepted by the student:

Group	Full name	Signature	Date
0AM0M	Asiamah Samuel Yaw		

TASK FOR SECTION
«SOCIAL RESPONSIBILITY»

For a student:

Group	Full name
0AM0M	Asiamah Samuel Yaw

School	Nuclear Science and Engineering	Department	Nuclear fuel cycle
Degree	Master programme	**Field of training/programme**	14.04.02. Nuclear physics and technology/ Nuclear medicine

Title of graduation thesis:

Physical and mathematical foundations of radiation diagnostics and therapy	
Initial data for section «Social Responsibility»:	
1. Information about object of investigation (matter, material, device, algorithm, procedure, workplace) and area of its application	Application area: The application of mathematics and nuclear physics in medicine.
List of items to be investigated and to be developed:	
1. Legal and organizational issues to provide safety: ▪ Special (specific for operation of objects of investigation, designed workplace) legal rules of labor legislation; ▪ Organizational activities for layout of workplace.	▪ Labour code of Russian Federation #197 from 30/12/2001 GOST 12.2.032-78 SSBT ▪ Sanitary Rules 2.2.2/2.4.1340-03. Hygienic requirements for PC and work with it
2. Work Safety: 2.1. Analysis of identified harmful and dangerous factors 2.2. Justification of measures to reduce probability of harmful and dangerous factors	▪ Insufficient illumination of workplace ▪ Excessive noise ▪ Deviation of microclimate indicators ▪ Electric shock
3. Safety in emergency situations:	▪ Fire safety;

Date of issuance of the task for the section according to the schedule	

The task was issued by consultant:

Position	Full name	Academic degree, academic rank	Signature	Date
Associate Professor	Perederin Yu.V.	Ph.D		

The task was accepted by the student:

Group	Full name	Signature	Date
0AM0M	Asiamah Samuel Yaw		

TOMSK POLYTECHNIC UNIVERSITY ТОМСКИЙ ПОЛИТЕХНИЧЕСКИЙ УНИВЕРСИТЕТ

Министерство науки и высшего образования Российской Федерации
федеральное государственное автономное
образовательное учреждение высшего образования
«Национальный исследовательский Томский политехнический университет» (ТПУ)

School of Nuclear Science & Engineering
Field of training (specialty): 14.04.02 Nuclear Science and Technology
Specialization: Nuclear medicine
Level of education: Master degree program
Nuclear Fuel Cycle Division
Period of completion: spring semester 2021/2022 academic year

Form of presenting the work:

Master Thesis

SCHEDULED ASSESSMENT CALENDAR
for the Master Thesis completion

Deadline for completion of Master's Graduation Thesis:	06.06.2022

Assessment date	**Title of section (module) / type of work (research)**	**Maximum score for the section (module)**
27.01.2022	Compilation and approval of technical tasks	
24.02.2022	Selection and research of materials on the topic	
15.03.2022	Review of the literature on the research topic.	
13.04.2022	Obtaining necessary mathematical expressions	
05.05.2022	Analysis and conclusion	
31.05.2022	Preparation for graduation work defense	

COMPILED BY:
Scientific supervisor:

Position	**Full name**	**Academic degree, academic status**	**Signature**	**Date**
Associate Professor	Konstantin Brazovsky	Ph.D. Professor (ISHKHBMT)		

APPROVED BY:

Program Director	**Full name**	**Academic degree, academic status**	**Signature**	**Date**
Nuclear Power Engineering / Nuclear medicine.	Vera V. Verkhoturova	PhD		

Abstract

The master's dissertation consists of (118) pages; (31) figures; (25) table; (71) references.

Keywords: simulations, beam, tomography, nuclear, industries, computed, X-rays, reconstruction, algorithm, development.

The objective of this study is to analyse the implications of complex mathematics in medical imaging using analytical concept of projections and reconstructions techniques in Radon transform, Fourier analysis, integral equations and sampling theory.

Coding and simulations performed in this research were conducted with the use of the Matrix Laboratory software (MATLAB) and Wolfram Mathematica. As a result of the research, the goal was to study the mathematical, physical, geometrical and algorithmic understanding of medical imaging.

The application of mathematics and nuclear physics in medicine is gaining momentum in the contemporary world. Mathematics is being applied in several medical fields: cardiovascular diseases, clinical schedules and tests, biofluids, genetics, and epidemiology. Nuclear physics in medicine involves using radiation to diagnose, treat and prevent diseases.

Nuclear medicine is rapidly developing, with the optimization of therapy and diagnostics requiring numerous calculations. The use of radioactive resources in cancer treatment and management, especially in shrinking tumors, killing cancerous cells and tissues, and reducing pain, requires accurate calculation and measurement of radioactive decay, isotopes, and other processes.

This research analyses the implications of complex mathematics in nuclear medicine. It highlights that numerical methods should be viewed in a more pragmatic light because key biomedical engineering principles are based on rigorous mathematical foundations.

Contents

Introduction

The underlying premise of this review is this basic yet sometimes overlooked reality. While radiation treatment "lives" at the crossroads of several disciplines, it is likely the most reliant on physics. This includes not just relying on clinical physics to ensure that radiation is provided safely and precisely, but also relying on the science and research side of physics in general, and medical physics in particular.

Advanced mathematics and physics have quietly crept into many fields over the last few decades. Aspects of our daily lives from cellular phones and satellite positioning systems to online banking and metal detectors, mathematics is at the core of technology. Perhaps no technology has had a more positive and profound impact on our lives than medical imaging, and no technology has a more prominent or underappreciated role for mathematics. The ability to more accurately concentrate and deliver radiation to the tumor target volume has accounted for much of radiation therapy's tremendous success over the last century. This progress has been fueled in large part by physics discoveries and technological innovations. However, there is still plenty of space for potential physics-based developments, such as image guidance and as well as four-dimensional motion control and particle therapy, as well as improved performance of smaller, less expensive technologies. The success of physics in radiation therapy has been based on the continued “fueling” of the field with new discoveries and inventions from physics research. The use of X-ray tomography, ultrasound, positron emission tomography, and magnetic resonance imaging has revolutionized medical practice. A mathematical and physics model for interpreting measurements and a computational algorithm for reconstructing an image are at the heart of each modality. Although each modality works on a different physical theory and probes a different aspect of our anatomy or physiology, the mathematics is used to model the measurements, develop reconstruction algorithms, and analyze the effects of noise are exceptionally similar. This text contains systematic instructions for understanding the various mathematical and physics concepts in nuclear medicine.

Chapter 1. Literature Review

With the introduction of faster, more accurate, and less harmful equipment in the last decade, medical imaging has undergone a revolution. This has prompted the creation of related software, which has in turn fueled the development of novel signal and image processing methods. Many of these methods are based on partial differential equations and curvature-driven flows, which are the primary subjects of this survey study.

1.1 What is radiotherapy?

One of the most potent and cost-effective curative treatments for cancer is radiotherapy, which is a very effective deoxyribonucleic acid-damaging agent with precise and specific effects on tumor. With breakthroughs such as intensity modulated radiotherapy (IMRT), image-guided radiotherapy (IGRT), and stereotactic ablative body radiation, it is a technology-driven treatment modality that provides genuine improvements in patient outcomes (SABR, formerly stereotactic body radiotherapy; SBRT) [1]. A computerized axial tomography (CAT or CT) scan is generated from a set of thousands of X-ray beams, consisting of 160 or more beams at each of 180 directions. To comprehend this large collection of X-rays, we must first understand just one beam. [1]. When a single X-ray beam of known intensity passes through a medium, such as muscle or brain tissue or an ancient Egyptian sarcophagus, some of the energy present in the beam is absorbed by the medium and some passes through. The intensity of the beam as it emerges from the medium can be measured by a detector. The difference between the initial and final intensities tells us about the ability of the medium to absorb energy. For the sort of X-rays, one might get at the dentist's office or for a suspected broken bone, the detector is a piece of film. A fan- or cone-shaped set of X-rays is emitted from a machine and those photons that are not blocked or absorbed by teeth or bone expose the film, thus creating a picture of the medium. The picture essentially lacks depth since anything positioned behind a point where the photons are blocked will not be seen. This shortcoming highlights a significant difficulty in imaging, namely, that the medium

through which the X-rays pass is not homogeneous. Muscles, for example, are fibrous and denser in certain areas than others; brain tissue is made up of grey matter, water, blood, neurons, and more; and a mummified, partially decomposed body, as well as the remains of artifacts interred with the deceased, is found inside the sarcophagus. The concept behind the CT scan is that by monitoring variations in the intensity of X-ray beams travelling through the medium in different directions and comparing the results, we may be able to discern which areas of the medium are more absorbent or less absorbent than others. [1].

1.2 Contributions of Physics and Mathematics to Medical Imaging and Radiotherapy

Only by carefully selecting physical variables can a link between physics and medicine be built. The specification of the physical quantity of absorbed radiation dosage, i.e. the energy imparted per unit mass, measured in gray units, is a critical component of radiation treatment success. In basic geometric or anthropomorphic phantoms, the radiation dose can be simply evaluated in three dimensions. Convolution/superposition or Monte Carlo methods can be used to calculate it with high accuracy in the patient. As a result, physicists can utilize computer models in conjunction with phantom measurements to design, test, and validate new approaches for enhanced dose localization and get an answer relatively instantaneously.

The discovery of X-rays by Wilhelm Conrad Röntgen in 1895 marks the beginning of physics in radiation therapy. This discovery is perhaps the most significant of physics' many "gifts" to medicine. Soon after their discovery, the immense potential of X-rays was recognized, not just for medical imaging but also for disease care. The first patient treatment with X-rays occurred only 1 year after the discovery. Thus, a physics discovery launched the field of radiation therapy. In radiation therapy, the main goal of physics has always been to improve the precision and accuracy of dose delivery to the (tumor) target

volume. In this area, remarkable progress has been made, based on four cornerstone innovations.

1. Fundamental discoveries leading to new treatment and imaging modalities.
2. Technology inventions in radiation dose delivery.
3. Technology inventions in treatment planning.
4. Technology inventions in imaging.

Finally, the paper establishes the contributions that advancement in mathematics and physics offers in medicine, especially in diagnosing, monitoring, managing, and treating terminal illnesses.

1.3 Physics of x ray production

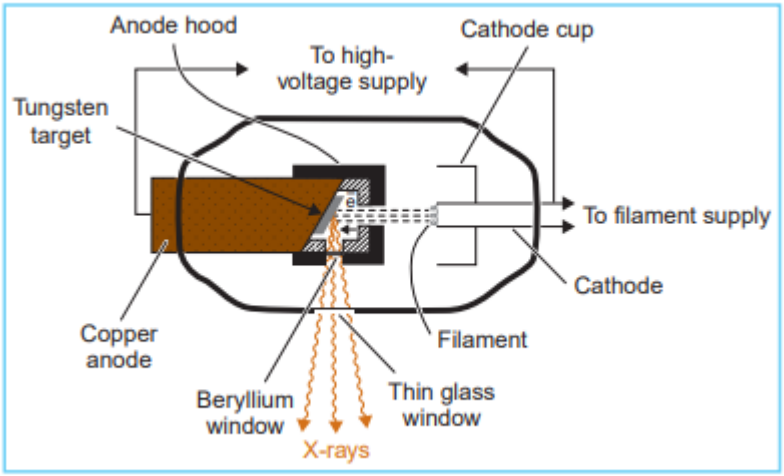

Figure 1.1 schematic diagram of a therapy x ray tube with a hooded anode.

The tube is made up of a glass envelope that has been vacuum-sealed. A cathode (negative electrode) and an anode (positive electrode) are hermetically sealed in the tube at one end. The cathode is a tungsten filament that emits electrons when heated, a phenomenon called thermionic emission. The anode is made out of a thick copper rod with a small tungsten target attached to the end. The electrons emitted from the filament are accelerated toward the anode and acquire high velocities before striking the target when a high voltage is supplied between the anode and the cathode. The x-rays are created by the electron deflection or acceleration caused by the tungsten nucleus's attractive force.

In Section 3.5, the physics of x-ray production will be explored. The x-ray beam enters the tube envelope through a tiny glass window. Thin beryllium windows are employed in some tubes to lessen the x-ray beam's natural filtering.

There are two ways of which x-rays are produced. One gives rise to bremsstrahlung x-rays and the other characteristic x-rays.

a. Bremsstrahlung

The result of a radiative "collision" between a high-speed electron and a nucleus is bremsstrahlung (braking radiation). The electron may be deflected from its direction by Coulomb forces of attraction and lose energy as bremsstrahlung, a phenomenon predicted by Maxwell's general theory of electromagnetic radiation, when moving near a nucleus.

According to this theory, energy is propagated through space by electromagnetic fields. As the electron, with its associated electromagnetic field, passes in the vicinity of a nucleus, it suffers a sudden deflection and acceleration. As a result, a part or all of its energy is dissociated from it and propagates in space as electromagnetic radiation. The mechanism of bremsstrahlung production is illustrated in Figure 1. Since an electron may have one or more bremsstrahlung interactions in the material and an interaction may result in partial or complete loss of electron energy, the resulting bremsstrahlung photon may have any energy up to the initial energy of the electron. Also, the direction of emission of bremsstrahlung photons depends on the energy of the incident electrons.

b. Characteristic X rays

X-rays are emitted when electrons interfere with the target. Figure 2 depicts the process by which they are made. An electron with kinetic energy E0 can interact with target atoms by ejecting an orbital electron, such as a K, L, or M electron, leaving the atom ionized. The collision will cause the original electron to recede with energy

$E_0 - E$, where E is the energy provided to the orbital electron. A portion of E is used to overcome the electron's binding force, and the remainder is borne by the ejected electron. When a hole in an orbit occurs, an outer orbital electron falls down to fill the

void. In so doing, the energy is radiated in the form of electromagnetic radiation. This is called characteristic radiation, i.e., characteristic of the atoms in the target and of the shells between which the transitions took place. (F. M Khan et al, 2014)

$Eph = -Ei\ Ej$ for allowed transitions:

$$\Delta n \neq 0;$$

$$\Delta l = \pm 1;$$

$$\Delta j = 0, \pm 1.$$

1.4 Types of radiation used in radiotherapy

Ionizing radiation - it forms ions (electrically charged particles) in the cells of the tissues it passes through. It creates ions by removing electrons from atoms and molecules.

Ionizing radiation can be sorted into 2 major types:

- Photon radiation (x-rays and gamma rays)
- Particle radiation (such as electrons, protons, neutrons, carbon ions, alpha particles, and beta particles)

(American Cancer Society, October 2014)

Non-ionizing such as radio waves, microwaves, and visible light waves are called. They don't have as much energy and are not able to form ions.

1.4.1 Ionization

Ionization is the process by which a neutral atom acquires a positive or a negative charge. Ionizing radiations can strip electrons from atoms as they travel through media. An atom from which electron has been removed is a positive ion. In some cases, the stripped electron may subsequently combine with a neutral atom to form a negative ion. The combination of a positively charged ion and a negatively charged ion (usually a free electron) is called an ion pair. Charged particles such as electrons, protons, and a-particles

are known as directly ionizing radiation provided, they have sufficient kinetic energy to produce ionization by collision1 as they penetrate matter. Ionizing photons interact with the atoms of a material or absorber to produce high-speed electrons by three major processes: photoelectric effect, Compton Effect, and pair production.

1.5 Imaging Techniques

1.5.1 Computed Tomography

A C.T. scanner, which stands for Computerized Tomography, is an important medical device that is frequently utilized in many hospitals. Understanding the definition of computerized tomography might help you understand what these scans are all about. Tomography is a technique for displaying a cross section through a human body or other solid object using x-rays or ultrasound. Computerized simply refers to data collection and processing by a computer, whereas tomography is a technique for displaying a cross section through a human body or other solid object using x-rays or ultrasound. In other words, a C.T. scan uses x-rays that are shot linearly through the human body along multiple positions or angles. The analysis of the x-rays passing through each line is reconstructed into a 2-dimensional cross section by a computer with the data collected by the paths of the x-rays, this gives rise to the term tomographic reconstruction.

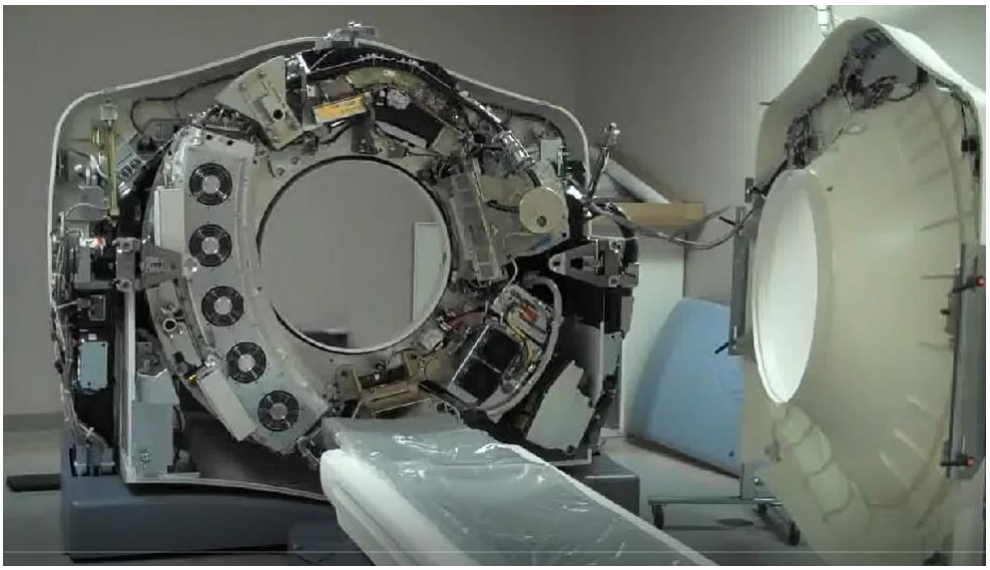

Figure 1.2 A typical modern medical CT scanner

A narrow beam of x-rays scans across a patient in synchrony with a radiation detector on the patient's opposite side in CT. The distribution of attenuation coefficients within the layer can be calculated if a significant number of transmission measurements are conducted at different orientations of the x-ray source and detector (Fig. 1. 3). A picture can be rebuilt that represents diverse structures with variable attenuation qualities by assigning different levels to different attenuation coefficients. A CT picture is a representation of attenuation coefficients like the image below.

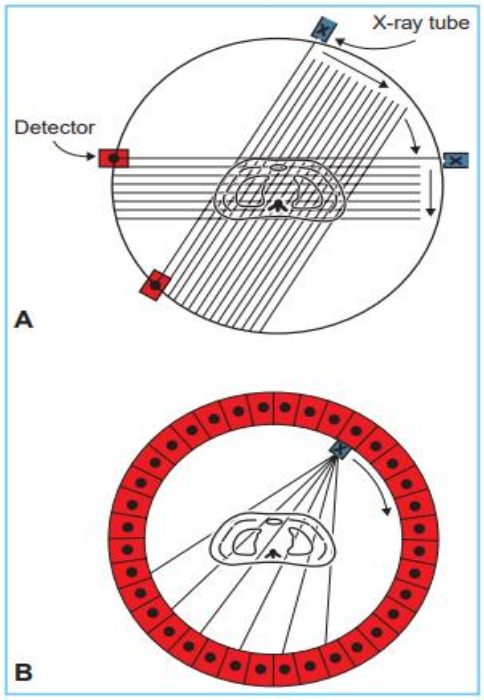

Figure 1.3 – Illustration of scan motions in computed tomography:
A. An early design in which the x-ray source and the detector performed a combination of translational and rotational motion; B. A modern scanner in which the x-ray tube rotates within a stationary circular array of detectors.

There has been considerable growth in both software and technology since CT scanning was debuted nearly 40 years ago. The majority of the hardware changes were made to reduce scan time by improving scanner motion and increasing the number of detectors. The x-ray tube revolves within a circular array of 1,000 or more detectors in Figure 1.1B, which depicts a modern scanner. Scanning times of 1 second or less are

possible with these scanners. A typical CT scan is shown in Figure 1.4. The x-ray tube spins around the patient in a slice-by-slice CT scanner to image one slice at a time. The x-ray tube spins axially around the patient in a spiral or helical CT scanner while the patient is transported longitudinally via the scanner aperture. Multiple detector rings are used in this scanner to scan numerous slices during each gantry rotation.

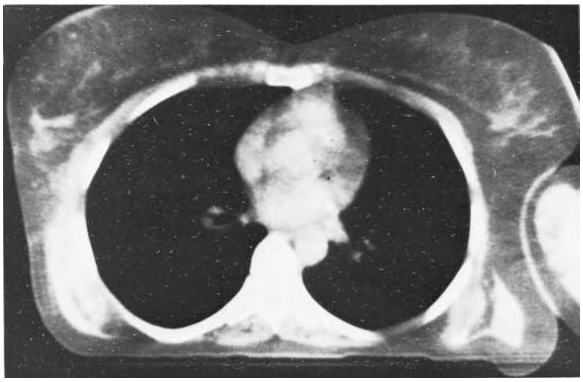

Figure 1.4 – a typical computed tomography image

1.5.2 Magnetic resonance imaging

Mansfield in 1977 saw the first cross-sectional MRI image of a student's finger using a small scale machine. This opened doors to funding, allowing them to build a full-size machine. Mansfield had his abdomen scanned using line-scan MRI. Interestingly, no one was brave enough to have a scan due to fear of the magnetic field inducing a myocardial infarction. A significant flaw in Mansfield's eyes was the speed with which an MRI produces images, and in 1977 he invented a technique where fast switching magnetic field gradients could be used to form an image significantly faster, known as echo-planar imaging. The first clinical scanner was built in 1980 and made available for clinical use in 1984. In 1963 Lauterbur joined the State University of New York (SUNY), in Stony Brook, with tenure in the Departments of Chemistry and Radiology, becoming a full professor in 1984. His main research focus was NMR spectroscopy, analyzing the composition of molecular structures, solids and liquids. Reid 23 In 1971 after reading an article by Raymond V Damadian, Lauterbur became interested in the potential biological

usages of NMR. Researchers had already shown that NMR could be used to distinguish malignant from non-diseased tissues or to assess blood flow. Until this time scientists had employed a uniform magnetic field, but Lauterbur realized that using a non-uniform field would allow the precise localization of structures within a sample to be determined. One of the first NMR images he took was of a clam. In 1973 he successfully published his seminal paper on MRI in Nature (an earlier draft was rejected). In this paper Lautebur coined the term "zeugmatography" for MRI. As he explained the word was derived from the Ancient Greek ζευγμα (zeugma) 'that which joins together'.

MRI has developed, in parallel to CT, into a powerful imaging modality. Like CT, it provides anatomic images in multiple planes. Whereas CT provides basically transverse axial images (which can be further processed to reconstruct images in other planes or in three dimensions), MRI can be used to scan directly in axial, sagittal, coronal, or oblique planes. This makes it possible to obtain optimal views to enhance diagnostic interpretation or target delineation for radiotherapy. Other advantages over CT include not involving the use of ionizing radiation, higher contrast, and better imaging of soft tissue tumors. Some disadvantages compared with CT include lower spatial resolution; inability to image bone or calcifications; longer scan acquisition time, thereby increasing the possibility of motion artifacts; and magnetic interference with metallic objects. The above cursory comparison between CT and MRI shows that the two types of imaging are complementary.

Basic physics of MRI involves a phenomenon known as nuclear magnetic resonance (NMR). It is a resonance transition between nuclear spin states of certain atomic nuclei when subjected to a radiofrequency (RF) signal of a specific frequency in the presence of an external magnetic field. The nuclei that participate in this phenomenon are the ones that intrinsically possess spinning motion (i.e., have angular momentum). These rotating charges act as tiny magnets with associated magnetic dipole moment, a property that gives a measure of how quickly the magnet will align itself along an external magnetic field. Because of the spinning motion or the magnetic dipole moment, nuclei align their spin axes along the external magnetic field (H) as well as orbit or precess around it (Fig.

1.5) [37]. The frequency of precession is called the Larmor frequency. A second alternating field is generated by applying an alternating voltage (at the Larmor frequency) to an RF coil. This field is applied perpendicular to H and rotates around H at the Larmor frequency. This causes the nuclei to precess around the new field in the transverse direction. When the RF signal is turned off, the nuclei return to their original alignment around H.

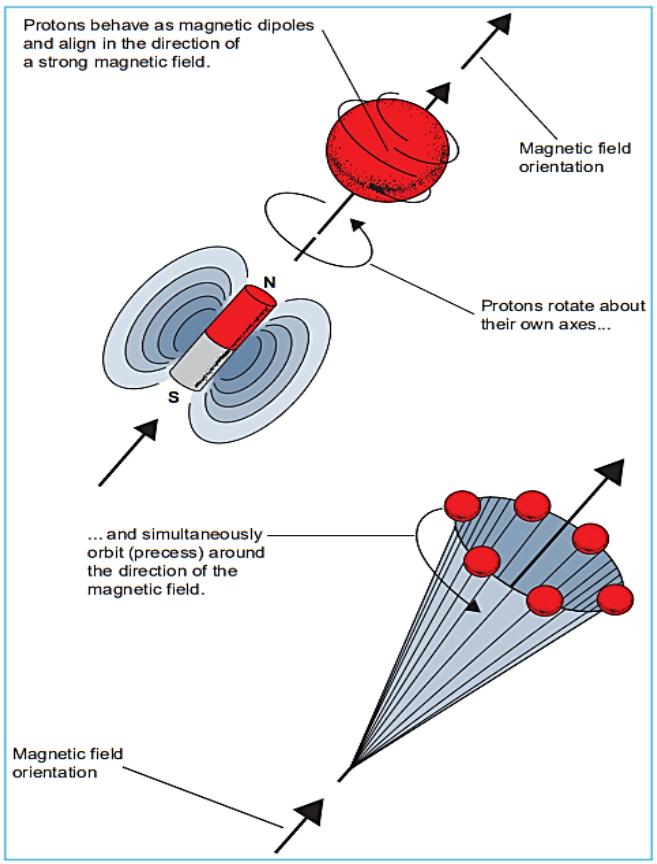

Figure 1.5 – Alignment and precession of protons in a strong magnetic field

This transition is called relaxation. It induces a signal in the receiving RF coil (tuned to the Larmor frequency), which constitutes the NMR signal. The turning off of the transverse RF field causes nuclei to relax in the transverse direction (T2 relaxation) as well as to return to the original longitudinal direction of the magnetic field (T1 relaxation). This is schematically illustrated in (Figure 1.6) [37]. The relaxation times, T1 and T2, are actually time constants (like the decay constant in radioactive decay) for the exponential function that governs the two transitions. The signal source in MRI can be any nucleus

with nonzero spin or angular momentum. However, certain nuclei give larger signal than the others. Hydrogen nuclei (protons), because of their high intrinsic sensitivity and high concentration in tissues, produce signals of sufficient strength for imaging. Other possible candidates are ^{31}P, ^{23}Na, ^{19}F, ^{13}C, and ^{2}H. Most routine MRI is based exclusively on proton density and proton relaxation characteristics of different tissues. Localization of protons in a 3-D space is achieved by applying magnetic field gradients produced by gradient RF coils in three orthogonal planes. This changes the precession frequency of protons spatially, because the MR frequency is linearly proportional to field strength. Thus, by the appropriate interplay of the external magnetic field and the RF field gradients, proton distribution can be localized.

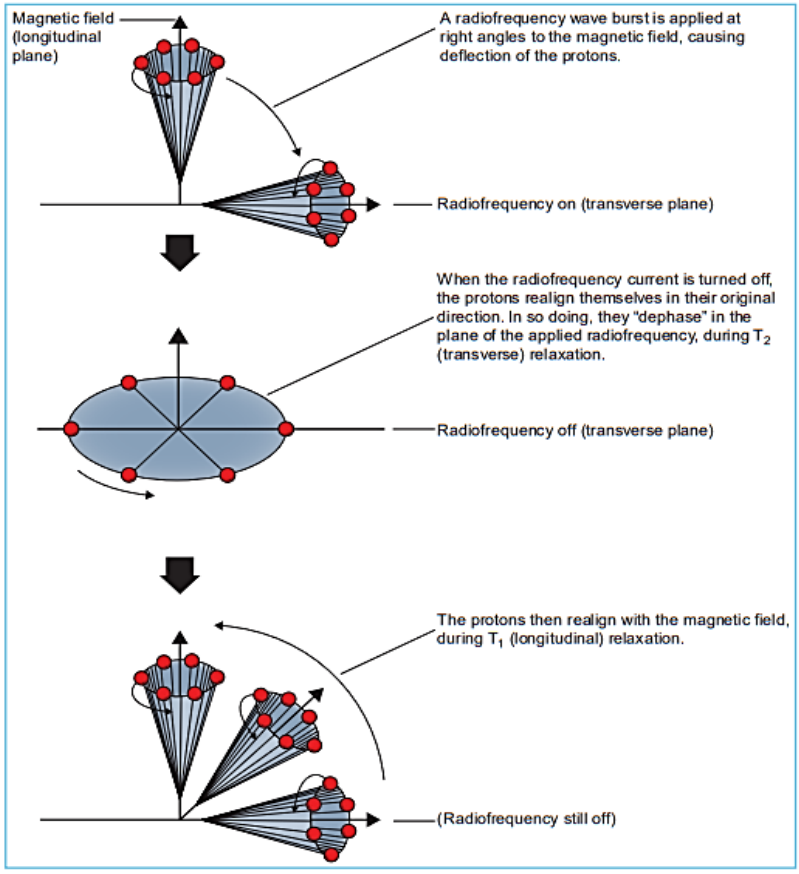

Figure 1.6 – Effects of radiofrequency applied at right angles to the magnetic field

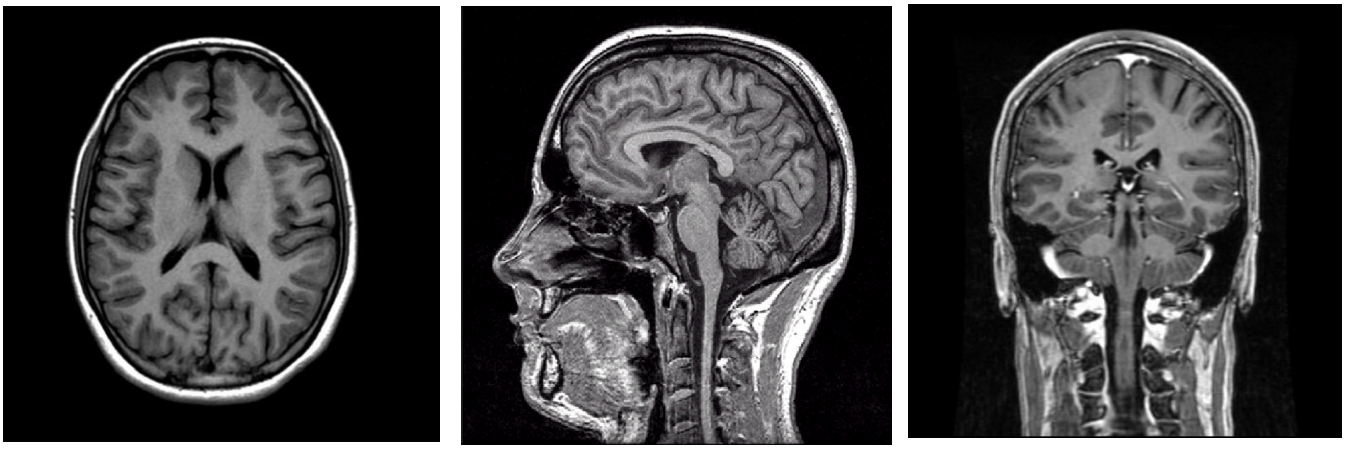

Figure 1.7 – Examples of MR images obtained in the axial, sagittal, and coronal planes of the human brain

1.5.3 Positron Emission Tomography

A P.E.T. scan, or Positron Emission Tomography scan, is a type of computed tomography scan that is commonly used for diagnostic purposes. P.E.T. creates images by sensing the energy emitted by radioactive isotopes decaying.

Isotopes are atoms of the same element with the same number of protons (positively charged particles) but a varying number of neutrons in the nucleus (neutral particles). Because radioactive isotopes are unstable, they emit positrons that hit with electrons and produce gamma rays that go in virtually opposite directions. This is known as pair annihilation.

PET systems use electronic collimation to establish the initial collision point by comparing the trajectories of the two observed gamma rays. The scanners encircle the patient with a circular sequence of gamma ray detectors to detect both gammas, allowing the instrument to employ electronic collimation to determine where the energy signal originated (Figure 1.8).

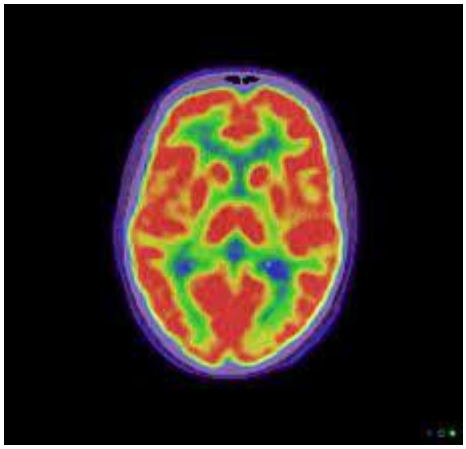

Figure 1.8 – Examples of PET images obtained in the axial of the human brain

Chapter 2.0 Theoretical aspect of medical imaging process

2.1 Mathematics and Equations That Govern Physics in Nuclear Medicine

A. Radioactive Decay and Nuclide Uptake

Nuclear medicine is continually evolving, and optimizing therapy and diagnostics necessitates a large number of computations. The use of radioactive materials in cancer treatment and management necessitates precise calculations and measurements of radioactive decay, isotopes, and other processes, particularly in shrinking tumors, eliminating malignant cells and tissues, and lowering pain. The rate of radioactive decay (A) is directly proportional to the number of atoms of the nuclide and its decay constant, λ (Świętaszczyk & Pilecki, 2013).

Therefore, the calculation of the radioactive decay is indicated by formula $A = \lambda N$ where A refers to total activity. An equation for determining the number of atoms in nuclide one (1) after the time (t) when the number of atoms at the beginning is t=0 is shown (Figure 2.1) below, representing a simple radioactive decay equation:

$$N_t = N_0 e^{-\lambda_1 t} \tag{2.1}$$

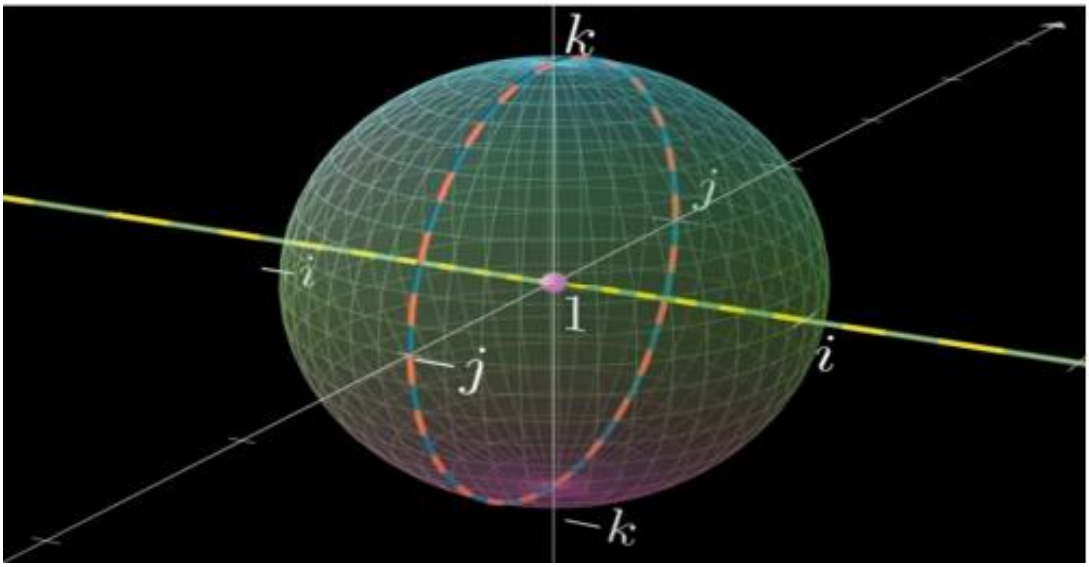

Figure 2.1 – Stereographically Projected Model of Quaternion Multiplication

Successive radioactive decay describes a decay of nuclide 1 that produces nuclide two and many others, as shown in the sequence below:

$$\text{nuclide 1} \rightarrow \text{nuclide 2} \rightarrow \text{nuclide 3}$$

The equation for the n-th nuclide is:

$$N_n(t) = N_1 0.{\lambda_1}^{-1}.N_n(t) = N_1 0.{\lambda_1}^{-1}.\sum_{i=1}^{n}\lambda_i\alpha_i e^{-\lambda_1 t}, \quad (2.2)$$

where $\alpha_i = \prod_{j=1}^{n}\frac{\lambda_j}{\lambda_j-\lambda_i}$

Under certain assumptions, such as assuming that the decay constants for all nuclides in a particular chain are the same, similar equations can be obtained for the activity of the n-th nuclide, the number of atoms in the second nuclide, and other parameters. Calculating radionuclide uptake is also an important part of putting this concept into practice as a medical approach. First, background radiation is estimated by creating the first region of interest (ROI) over a target organ and the second in the vicinity of the organ. The formula below allows for the calculation of nuclide uptake;

$$uptake = \frac{patient-background}{nuclide-background}(100\%) \quad (2.3)$$

B. Complex Numbers and Quaternions in Medicine Imaging

Complex numbers and quaternions in medicine are utilized in performing CAT scans using the X-ray principle. Conventional 2- dimensional complex numbers are expressed in the form a + bi, where a and b are real numbers, and i represents the fundamental unit of an imaginary number($\sqrt{-1}$). Quaternions are a 4-dimensional extension of traditional 2-dimensional complex numbers and are expressed in the general form:

$$z = bi + cj + dk, \quad (2.4)$$

where a, b, c, d are real numbers and i, j, k, are distinct square roots of -1.

Complex numbers and quaternions are used in the geometry of CT scans and X-ray imaging. Because X-rays are attenuated at different levels as they move through the body, and MRI and CT scans undertake hard 3-dimensional transformations, is it possible to express this with quaternions? Each quaternion is iterated as a computed interpolated change for location and orientation. In addition, the interpolated rotation is a small-angle approximation of a rotation quaternion that is linear in three parameters (Carter, 2003). It

is essential to parametrize ax + by = c in a radon transform representing trajectories of different beams entering the body when conducting CT scans and X-ray imaging. The parametrization of lines ax + by = c uses a, b and c as constants as shown below:

$$\frac{a}{\sqrt{a^2+b^2}}x + \frac{b}{\sqrt{a^2+b^2}}y = \frac{c}{\sqrt{a^2+b^2}}, \quad (2.5)$$

whereby the two coefficients, $\frac{a}{\sqrt{a^2+b^2}}$, $\frac{b}{\sqrt{a^2+b^2}}$ Define a point on a unit circle. Thus, the angle θ corresponding to that point on the unit circle is calculated through:

$$\theta = \cos^{-1}\frac{a}{\sqrt{a^2+b^2}}, \quad (2.6)$$

C. Calculations in Medical Imaging, Radiation, and Electromagnetics

In medical imaging, radiation, and electromagnetics, mathematical approaches are used through partial differential equations (PDEs). Methods based on PDE are popular for image processing have been popular in the previous years. For instance, a person can think of an image as a map I: D → C, i.e., to any point x in the domain D, I associate a "color" I(x) in a color space C. The algorithms can be used to deform the image into different shapes by introducing time (t) as shown in the formula:

$$\frac{\partial I}{\partial t} = F[I], \quad (2.7)$$

whereby I (x, t): D × [0, T) → C is the evolving image, F is an operator which characterizes the given algorithm, and the initial condition is the input image I0. According to Šagátová et al. (2020), the acceleration of the beams in radiation therapy is also calculated through mathematical calculations to determine their intensity.

2.1.1 CT

Acquisition of body contours and internal structures is best accomplished by 3-D volumetric imaging [computed tomography (CT), magnetic resonance imaging (MRI). The scans are performed specifically for treatment-planning purposes, with the patient positioned the same way as for actual treatment.

CT image reconstruction is a highly difficult mathematical technique that is carried out by a computer. The reader is directed to Brooks and Di Chiro's study for an overview

of various mathematical approaches for image reconstruction. Each axial plane is divided into small voxels by the reconstruction method, which creates CT numbers, which are related to the computed attenuation coefficient for each voxel. CT numbers typically begin at –1,000 for vacuum and end at 0 for water. The CT numbers normalized in this manner are called Hounsfield numbers (H):

$$H = \frac{\mu_{tissue} - \mu_{water}}{\mu_{water}} \times 1000, \quad (2.8)$$

where m is the linear attenuation coefficient.

Thus, a Hounsfield unit represents a change of 0.1% in the attenuation coefficient of water. The Hounsfield numbers for most tissues are close to 0, and approximately +1,000 for bone, depending on the bone type and energy of the CT beam.

Special treatment-planning CT scans are required with full attention to patient positioning and other details affecting treatment parameters. Some of the common considerations in obtaining treatment-planning CT scans are the following:

(a) A flat tabletop should be used; usually a flat carbon fiber overlay which closely mirrors the treatment couch is mounted in the CT cradle.

(b) A large-diameter CT aperture (e.g., ≥70 cm) can be used to accommodate unusual arm positions and other body configurations encountered in radiation therapy.

(c) Care should be taken to use patient-positioning or immobilization devices that do not cause image artifacts.

(d) Patient positioning, leveling, and immobilization should be done in accordance with the expected treatment technique or simulation if done before CT.

(e) External contour landmarks can be delineated using radiopaque markers such as plastic catheters; and (f) Image scale should be accurate both in the X and Y directions.

Method of Proofs

The fact that a CT scan is computerized is the most important aspect of it. All of the data is input into a computer, which is then examined using an algorithm to rebuild an image from x-ray photons. It is not necessary to look over these formulas in detail or to have a thorough comprehension of the mathematics; nonetheless, a general understanding

will sufficient for this work. The body is typically viewed as a sequence of two-dimensional cross sections termed slices in medical imaging and radiation. This means that each slice has a density f. (x,y). The function f(x,y) is unknown in medical imaging, and we wish to identify it to the greatest extent feasible using line integrals. For CT and PET, the line integral data corresponds to x-ray or -ray data, respectively. It is the radio wave that travels along a certain line in MRI. It's a photon beam in every scenario. We know what f(x,y) is in radiotherapy, and we want to blast a tumor with as little radiation as possible to surrounding healthy tissue. For Lines Parallel to the x-axis we have:

$$L(y) = \int f(x, y)\, dx. \tag{2.9}$$

While for lines parallel to the y-axis this becomes:

$$L(x) = \int f(x, y)\, dy. \tag{2.10}$$

For other directions, we need to parameterize the lines. Let θ be the angle as measured from the positive x-axis, and let $U\theta = \cos(\theta)\, \hat{\imath} + \sin(\theta)\, \hat{\jmath}$ be the unit vector in the direction θ. Given a point (x,y) with a position vector $V = xi + yj$ we define:

$$L(\theta,t) = \{(x,y) : V \cdot U\theta\ \theta = t\}. \tag{2.11}$$

For the point (a,b) parallel to U_θ we have $t = \sqrt{a\ b}$. Every other point (x. y) in L(θ, t) is on the line with 2 + 2 perpendicular vector $U\theta$ at a distance t from the origin. The Radon or X-ray transform of f(x, y) is obtained by integrating f(x,y) over the line L (θ,t).We write:

$$L(\theta,t) = \int f(x, y)\omega(\theta, t), \tag{2.12}$$

where the differential form $\omega(\theta, t) = \cos\theta\, dx + \sin\theta\, dy$.

Note $\theta = 0$ gives dx; $\theta = \pi/2$ gives dy.

We let polar coordinates fluctuate between 0 and 2. Because going from 0 to 2 would be redundant in our measurements and calculations, symmetry advises that we limit ourselves to angles between 0 and 2, with t indicating signed distance from the origin. To be precise, the data obtained by tomography is a set L(k, tm) that fluctuates over a finite number of k and m values. The transform data obtained for the density functions encountered in the body has the property that L(,t) is continuous in t except at a finite

number of places for each fixed. As such, it is the convention to think of L (θ_k, t) being known for all t in a given direction, this determines a profile.

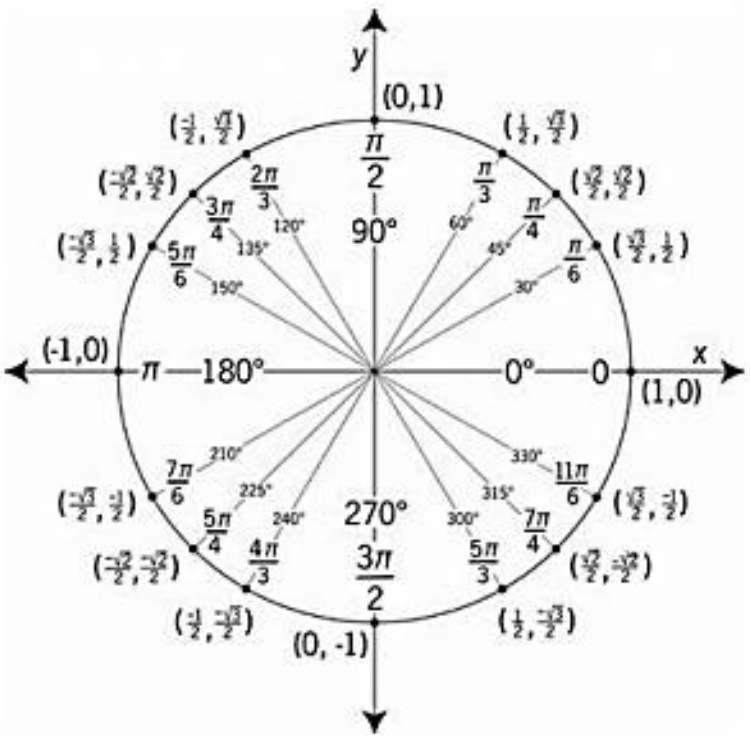

Figure 2.2 – Polar coordinates along 360 degrees

The other part of computing is eliminating errors and understanding what the photon beams being used do. A photon beam passes through or strikes a medium, traveling a total distance D through the medium. We write D = n Δs where n is very large and each increment of Δs is very thin. The probability of a photon being absorbed or scattered in each increment is p, the probability the photon gets through is $(1\text{-}p)^n$. For when Δs is sufficiently small, we have p close to zero. The approximation:

$$(e^{-p}) \approx 1\text{-}p. \tag{2.13}$$

Gives the probability of transmission:

$$(e^{-p})^{n} = e^{-pn} = e^{-\delta T}. \tag{2.14}$$

where δ is called the coefficient of attenuation for the material. The value of δ is proportional to the imaginary component of the refractive index. So by knowing the refractive index of materials we can predict the probability of the photons being

transmitted as well as reflected. Suppose it can be shown that the probability that a photon is reflected is:

$$p = \frac{(n-1)^2}{(n+1)^2}. \quad (2.15)$$

If we use the example of glass, with an index of refraction n = 1.5 and two surfaces we can determine the probability of reflection.

$$p = \frac{(1.5-1)^2}{(1.5+1)^2} = 0.4.$$

Double the probability of one surface to get the probability of the sheet of glass, and you'll notice that there's about a 0.08 chance of photons being reflected and a 0.92 chance of light being transmitted. This makes sense because we anticipate light to enter through our windows and not be reflected or absorbed by a higher index of refraction object. The photon beams travelling through the patient's body are subjected to this logic. The real data collected is beam attenuation, which is defined as the output to input ratio (I_0t/I). X-ray photon density is a measurement of how many photons are present in a given amount of time. Beer's Law states that I_0t/I is proportional to exp L(θ,t). To demonstrate this, we'll use a variant of Beer's Law: $I=I_0e^{-\mu x}$, where I is the detected x-ray intensity, I_0 is the beginning x-ray intensity, e is the materials linear attenuation coefficient, and x is the x-ray duration. $\mu = \ln(I_0/I)$ is a rearranged version of this equation. We get $e\mu = I_0/I$ when we reduce the natural log with exp, which is why I_0t/I is proportional to expL(θ,t).. Hounsfield values are proportional to beam attenuation Thus, H=900 is double the x-ray density of H=30. Some Hounsfield values are shown in the table 2.1 below:

Table 2.1 shows some Hounsfield values.

Material	Hounsfield Unit
Air	-1000
Lung	-500 to -200
Fat	-200 to -50
Water	0

Continuation of the Table 2.1

Blood	25
Muscle	25 to 40
Bone	200 to 1000

2.1.2 MRI

MRI's are an interesting piece of technology that can be hard to understand since it incorporates abstract ideas and techniques in order to function the way it does. To try and explain, this paper will try to only touch upon the key aspects that are most important in understanding how it works. To begin, the patient is going to be considered positioned in a uniform magnetic field B directed perpendicular to the body cross sections. Taking these cross sections to be parallel to the x-y plane, the magnetic field has direction k or -k. The field must be sufficiently strong to cause many of the hydrogen nuclei (protons) to align in its direction. Typically, this magnetic field has a magnitude 0.5 to 2.5 T. Due to quantum mechanical constraints on the possible angular momentum states, the protons cannot align exactly the same direction. They precess (wobble) about what we visualize to be a 30 degree angle, returning to random orientation once the field is removed.

The frequency of precession called the Lamour frequency, is given by:

$$F = \frac{\gamma|B|}{2R}. \tag{2.16}$$

where ɣ is the gyromagnetic ratio equal to $2.68(10)^8$ Hz/T for the hydrogen ion.

To attain a field that is nearly constant over the length of the body requires a Helmholtz coil. Wrapping N turns of wire radially in a circular loop of radius r induces a magnetic field perpendicular to the loop having maximum magnitude:

$$B = \frac{\mu_\circ NI}{2R}. \tag{2.17}$$

where I is the current, in amperes, in the wire and $\mu_0 = 4\pi(10)^{-7}$ Tm/A.

This field has the desired direction but decreases rapidly with distance. Adding another circular loop at a distance R from the first, and having the same values of N and

I, yields a Helmholtz coil. It can be shown that the superposition of the two fields is nearly constant between the coils. Since the patient must lie between the coils, a typical value of R is 2 or more meters. Since |B| $\mu_0 \leq$ NI/2R, the values of I and N must be very large to obtain Tesla level fields. We want $N \geq (10)^4$ and $I \geq. (10)^3$ .Since electrical resistance would require prohibitively high voltages, the circuit is super cooled using liquid nitrogen.

When the field is switched off, the protons emit photons at the Lamour frequency; this is the signal. For a one T field, we get 268 MHz, which fall in between the range of FM and cell phone frequencies. The energy of each photon is given by E= hf where h= $6.626(10)^{-34}$ Js, this is Planck's constant. In units of electron volts this is of order $(10)^{-6}$ eV which is quite safe for the patient. By comparison, UV radiation is 3 to 5 eV; for CT scan the photons are more than $(10)^5$ eV. Of course, if all the protons were emitting photons of the same frequency we could not determine different tissue. For this reason there are ordinary electromagnets called gradient coils that increase or decrease the field by 10 or 20 Gauss (1 Gauss = $(10)^{-4}$ T). Gradient coils in the z-direction allow us to identify x-y sections. Another gradient coil, say in the x-direction, provides a single frequency signal over the lines in the direction of the y-axis. Rotating the latter gradient coil gives lines in different directions. These determine the line integrals used for tomographic reconstruction of each f(x,y) section. In the simplest case, we obtain what is called a proton spin density picture. We can also measure relaxation time for the ions, taking advantage of the fact that is will be different for hydrogen in different compounds.

2.1.3 PET

PET signals are converted into three dimensional image slice with some assumptions of laws of conservation of momentum and energy.

$$P = MV, \tag{2.18}$$

where P is momentum, M is mass and V is the velocity of a given object.

To use this law with two objects colliding it is adapted to:

$$P_{total} = M_e V_e + M_p V_p, \tag{2.19}$$

where P_{total} is the total momentum and the masses and velocity are respectively assigned.

As a system, the pair has an initial kinetic energy of:

$$K_0 = \frac{1}{2} m {V_e}^2 + \frac{1}{2} m {V_p}^2. \tag{2.20}$$

The energy is raised by $2mc^2$ and the momentum is conserved after annihilation. However, because $2mc^2$ has a magnitude of $(10)^{-13}$ Joules and V_p and V_e have magnitudes of $(10)^5$ or $(10)^6$ m/s, K_0 is now presumed to be negligible. This implies that K_0 is on the order of $(10)^{-18}$ Joules, a very small value that can be overlooked. The final energy is: assuming the annihilation process produces exactly two photons, which almost usually happens in practice.

$$h\frac{c}{\lambda_1} + h\frac{c}{\lambda_2} = 2mc^2. \tag{2.21}$$

This indicates that wavelengths λ_1 and λ_2 are in the range of $(10)^{-12}$ m, implying the emission of gamma radiation. In comparison to $|h/\lambda_1|$ and $h/\lambda_2|$, the starting momentum of this system is likewise believed to be insignificant because,

$hc/\lambda = mc^2$ yields $h/\lambda = mc$,

which is far greater than $|mV|$.

Because the pair's initial momentum is essential zero, they must fly apart in order to retain a zero total vector momentum and sustain the conservation of momentum. The photons must travel in opposing directions at an angle of 180° apart and have identical momentum magnitudes. This indicates that

$$|h/\lambda_1| = |h/\lambda_2| \text{ so } \lambda_1 = \lambda_2. \tag{2.22}$$

Using this in the equation below that we acquired above:

$$h\frac{c}{\lambda_1} + h\frac{c}{\lambda_2} = 2mc^2 \ \ simplifies\ to \frac{hc}{\lambda} = mc^2 = \frac{h}{mc}. \tag{2.23}$$

This simplified equation gives the Compton wavelength, which is what makes PET scans possible.

2.2 Mathematics for linear Systems

An image can be represented as the convolution of a position-invariant point spread function within an object with specific limitations, allowing the Fourier transform theory to be used to describe imaging in a different way. We will look at the mathematics of sampling theory and model the implications of digitization of the medical image, as sampling is a key aspect in digital imaging.

2.2.1.0 The Radon transform

In order to work in the circular geometry of CT scans, it is helpful to parametrize lines $ax + by = C$ in $\mathbb{R}^2$ to a set of oriented lines with radial parameters $\ell_{t,\theta}$ in $\mathbb{R} \times S^1$ (see figure 2.2). In medical imaging, these lines are representative of the trajectories of x-ray beams entering a body. Consider the general line in $\mathbb{R}^2$:

$$ax + by = C, \tag{2.24}$$

where a, b, and c are constants. We then have

$$\frac{a}{\sqrt{a^2+b^2}}x + \frac{b}{\sqrt{a^2+b^2}}y = \frac{c}{\sqrt{a^2+b^2}}, \tag{2.25}$$

whereby the two coefficients, $\frac{a}{\sqrt{a^2+b^2}}$, $\frac{b}{\sqrt{a^2+b^2}}$ Define a point on a unit circle.

Thus, the angle θ corresponding to that point on the unit circle is calculated through:

$$\theta = \cos^{-1}\frac{a}{\sqrt{a^2+b^2}} \tag{2.26}$$

Then *cos* θ = $\frac{a}{\sqrt{a^2+b^2}}$ and *sin* θ =$\frac{b}{\sqrt{a^2+b^2}}$. This parametrization has an intrinsic repetitive quality; the angle θ can only take on values of [0, π) before repeating previously described lines. Let t be the distance from the origin to the line ax+by = c along the angle θ. Then the line can also be described as the set of solutions (x, y) to the inner product.

$$t = \langle (x, y), (\cos\theta\,, \sin\theta) \rangle = \langle (x, y), \omega \rangle. \tag{2.27}$$

Therefore, *t* is equal to the right side of equation (2.27). Notice that our definitions of *t* and θ also give us a point on the line, (*t cos θ, t sin θ*), where a line at angle θ.

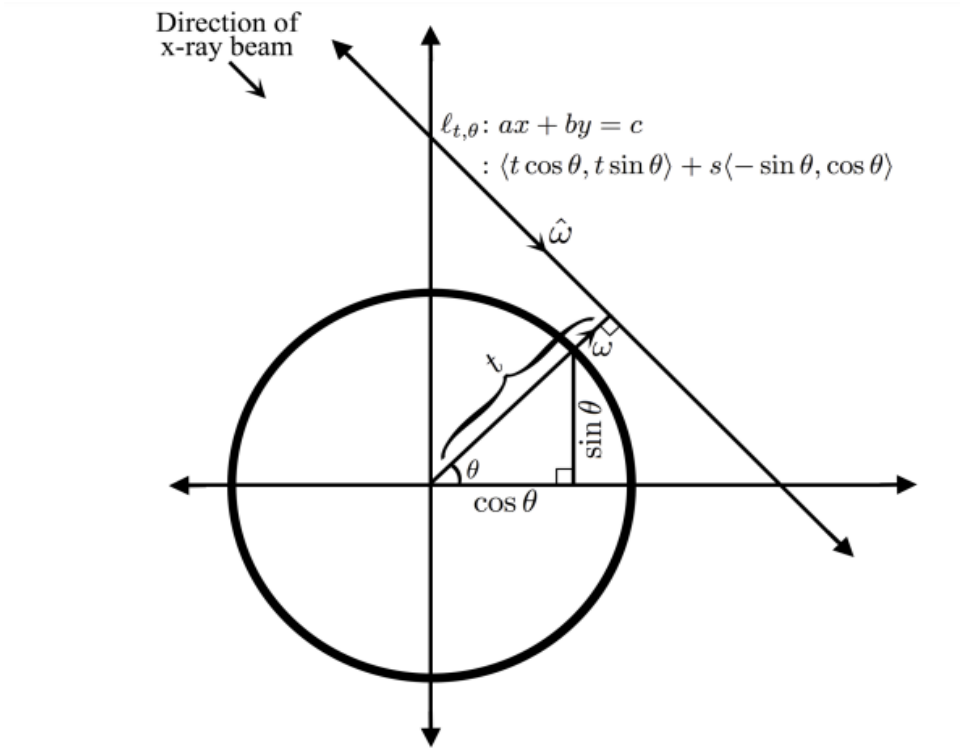

Figure 2.2 the parametrization of lines ax + by = c to lines $\ell_{t,\theta}$ in $\mathbb{R}^2$

Intersects $ax + by = C$ This intersection is a right angle, because while the slope of the line $ax + by = C$ is$-\frac{a}{b}$, the tangent of θ is

$$tan\,\theta = \frac{sin\,\theta}{cos\,\theta} = \frac{a}{b}. \tag{2.28}$$

Let the vector$\omega = \langle\cos\theta, \sin\theta\rangle$, perpendicular to the line $+by = C$, and let the vector $\hat{\omega} = \langle -\sin\theta, \cos\theta\rangle$ be parallel to this line. We can therefore create a vector equation in terms of *t* and θ for the line,

$$\ell_{t,\theta} = t_{\omega} + s_{\hat{\omega}}, \tag{2.29}$$

$$\ell_{t,\theta} = \langle t\,cos\,\theta, t\,sin\,\theta\rangle + s\,\langle -\sin\theta, \cos\theta\rangle,$$

where s ∈ ℝ This line is the same as the line ax + by = c, but the parametrization is in terms of an affine parameter t and the angular parameter θ, making it easier to determine a set of lines emanating from or passing through a single point.

2.2.1.1 Parallel projection

Depending on the type of equipment and settings used, multiple methods of gathering projections are used, such as parallel, fan-beam, and cone beam procedures. A projection is created by combining sets of line integrals for each ray. A parallel projection is the most basic and straight forward method of studying projections, and it entails collecting parallel ray integrals for a fixed angle. In Figure 2.3, the parallel projections are effectively depicted and discussed. The x-ray source and detector positions are altered in opposite directions along parallel lines of the object under inquiry during the projection process.

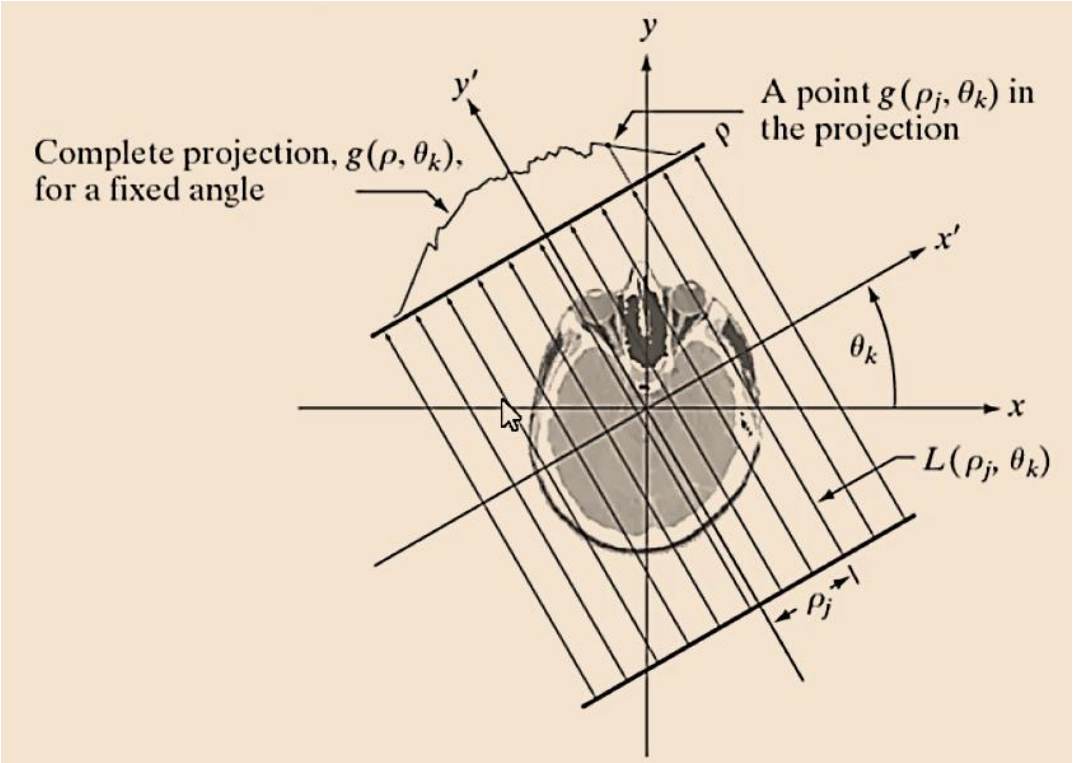

Figure 2.3 – Parallel beam projection showing the individual rays, angle of projection θ and projection view function $g(\rho, \theta_k)$

2.2.1.2 Numerical interpretation of the Radon forward transform

The numerical method of projection entails adding assigned pixel values in columns and rows, then converting the results into a sinogram as explained below. The data obtained from the detector during x-ray propagation is represented by numbers in an array.

According to the colors they represent, these values vary from 0 to 255. However, after flattening, the color codes in the grayscale images utilized in this study only range from 0 to 1, therefore each pixel is occupied by the range of values numerically shown below for the sake of explanations, while the simulation results are found in the next chapter.

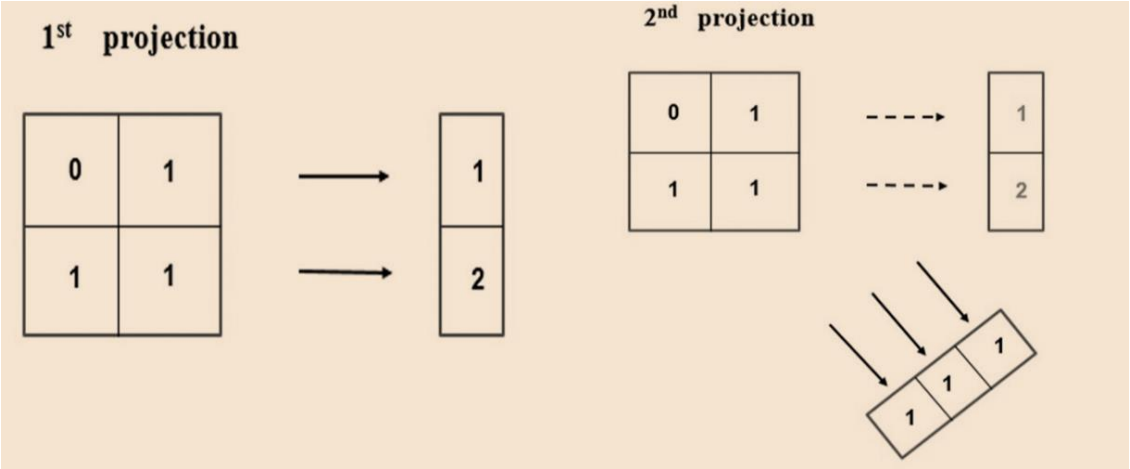

Figure 2.4 Numerical illustration on how projections are computed from 2-dimensional array to 1-dimensional array to form a sinogram

2.2.1.3 The Inverse Radon Transform and the back-projection

The inverse Radon transform is a technique for reconstructing a plane function from its integrals across all plane lines. This presents a solution to the difficulty of reassembling a body image from CT scan data. The Radon transform can be inverted using a variety of techniques, including Fourier transforms, the Central Slice Theorem, and functional analysis.

The Fourier slice theorem can be used to build an analytical approach to the inverse Radon transform. A one-dimensional Fourier transform of the Radon transform is related to a two-dimensional Fourier transform of the function, according to this theorem. The projection slice theorem can be used to convert a 2D object function into a 2D Fourier domain in tomography. This theorem is applicable to parallel beam computed tomography image reconstruction. The image reconstruction method is a classic inverse problem that produces an image from its projection data when applied. The following step is to retrieve

our genuine image after we receive a sinogram, because the sinogram does not make sense in terms of visibility of what we hope to get at the end.

Back-projection is the process of smearing all of the projection data back along the same route as the forward projection. As a result, an image is reconstructed as a result of this. A one-dimensional Fourier transform of the detector function at an angle, according to the Fourier slice theorem, is an exact duplicate as a line across the 2D Fourier representation of the entire object. As a result, it shows the line passing through the origin at the exact projection angle. As a result, a single line in the Fourier domain can be filled by measuring a single projection of an object, as shown in figure 2.5 below.

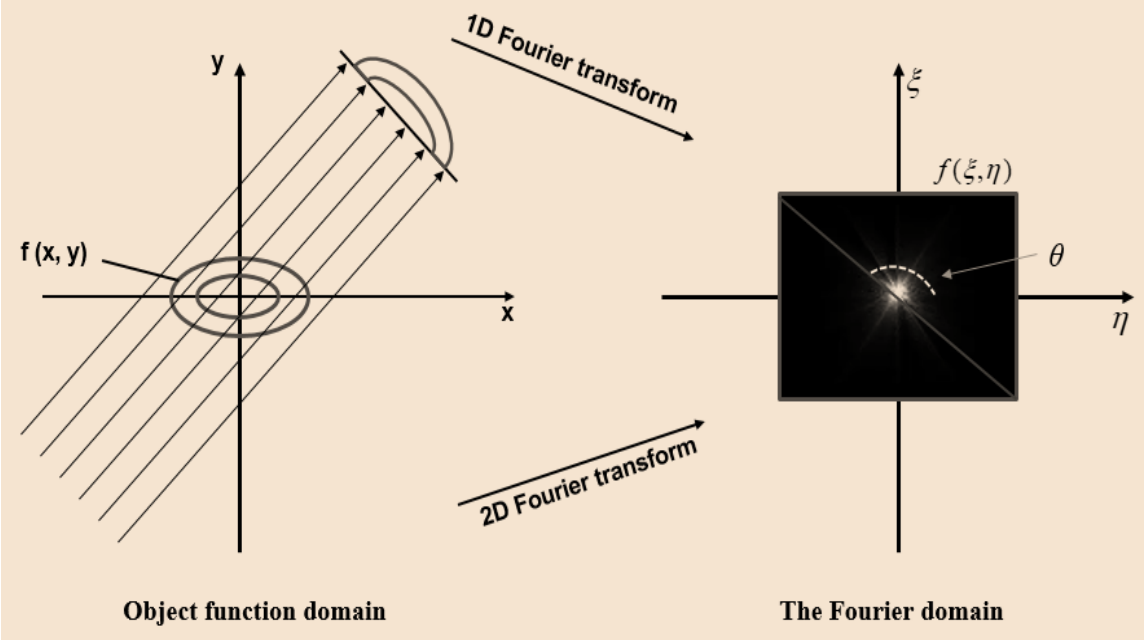

Figure 2.5 – Scheme of Fourier representation of a single projection.

Apparently, as the projection is collected from multiple angles and transforming it into the Fourier domain will result in obtaining a full Fourier representation as shown by the figure 2.6 below.

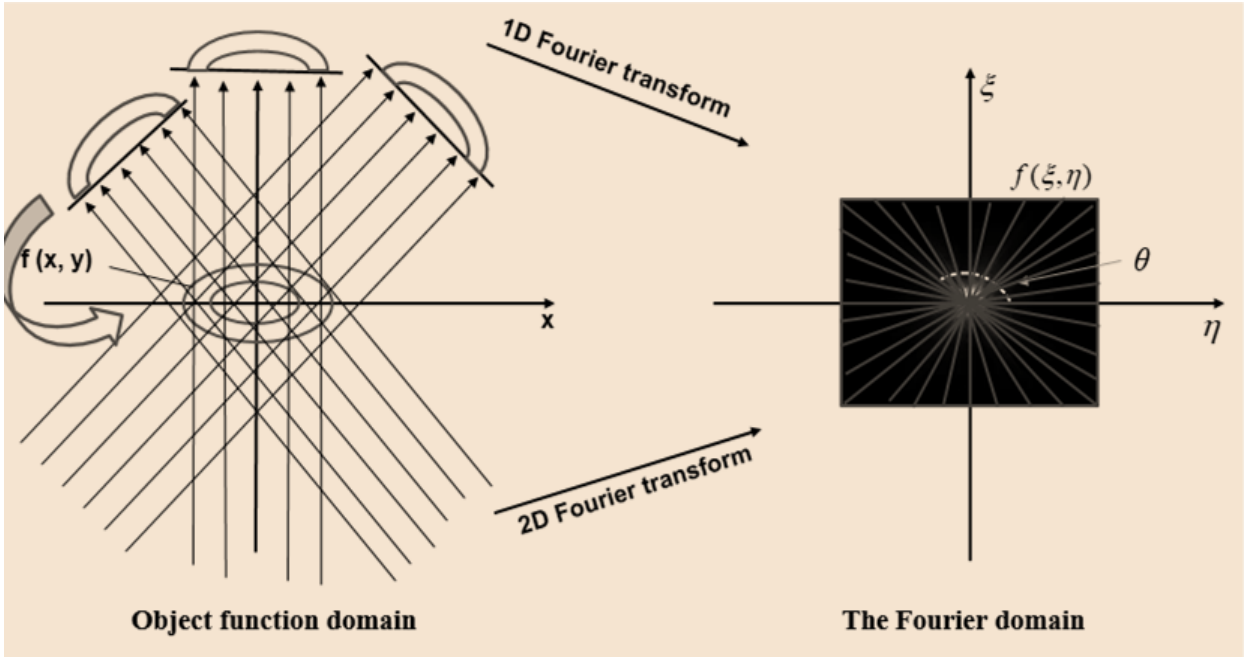

Figure 2.6 – Full Fourier scheme of projections taking from multiple angles

Fourier sample lies in circles rather than square grits, hence the pixel data must be interpolated into square grits. As seen in Figure 2.7, this is accomplished by interpolating from the Fourier domain to the frequency domain.

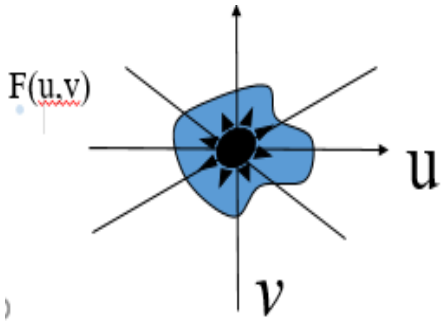

Figure 2.7 – Sketch of the frequency regions in the Fourier sampling domain

2.2.1.4 Unfiltered Back projection

Because it can model the data obtained from such scans, the Radon transform is useful for tomography applications like CT. Due to the fact that the data does not directly match the item being photographed, it is not immediately applicable to diagnostic applications. To employ tomographic technologies in the actual world, a way of reproducing the original image (or, in the case of the Radon transform, the original

function) with high specificity and authenticity is necessary. For continuous data (i.e., functions), perfect reconstruction using abstract inversion is conceivable, while finite (discrete) data accessible in the real world only allows for estimated reconstructions. As a result, the majority of work in CT and other real-world applications is focused on improving these estimations. Unfiltered back projection, which takes the average values of the function along each line and "smears" or projects them back along the line to generate an image, is an initially appealing method.

As unfiltered back projection's lack of specificity renders it unusable for medical imaging applications, we must examine other methods for inverting the Radon transform. The Radon transform is closely related to the Fourier transform, an extensively studied method whose inverse is well-described, by the Central Slice Theorem. We will introduce the Fourier transform before exploring this relationship further.

2.2.2 Dirac delta function

Dirac delta function $\delta(x)$, is defined as follows:

$$\delta(x) = \begin{pmatrix} +\infty & if\ x = 0 \\ 0 & if\ x \neq 0 \end{pmatrix}, \tag{2.30}$$

This has a unity integral value that is naturally unit less:

$$\int_{-\infty}^{+\infty} \delta(x)dx = 1. \tag{2.31}$$

With an implicit rather than explicit nod to Dirac, we'll name δ(x) a "delta function." This delta function has a number of unique characteristics. First, it is quite simple to demonstrate that when the delta function is present in the integrand with another function, it substantially simplifies integration:

$$f(0) = \int_{-\infty}^{+\infty} f(x)\delta(x)dx \tag{2.32}$$

If the product of a function and the delta function is integrated over the domain of the function, the result is the function's value at x = 0, providing the function exists. The above property can be generalized to yield a sample of f(x) at point x = x′:

$$f(x') = \int_{-\infty}^{+\infty} f(x)\delta(x - x')dx \tag{2.33}$$

Where δ(x − x′) is a shifted delta function, shifted from x = 0 to x = x′. A series of delta functions is called a “comb” or “shah” function, and these can be represented as a discrete sum since they do not overlap:

$$\mathrm{III}(x) = \sum_{n=-\infty}^{+\infty} \delta(x-n). \tag{2.34}$$

The above equation is an infinite sum of delta functions that are spaced at integer intervals (Note: n and x have the same units). When a function is multiplied by the comb function, it can be "point sampled" at integer intervals:

$$\mathrm{f(x)III}(x) = \sum_{n=-\infty}^{+\infty} f(x)\delta(x-n), \tag{2.35}$$

so that the sum of non-overlapping sampled function values f(x) for x = n produces the integral of this product:

$$\int_{-\infty}^{+\infty} f(x)\,\mathrm{III}(x)dx = \sum_{n=-\infty}^{+\infty} f(n) \tag{2.36}$$

2.2.3 Convolution

The convolution of f(x) with h(x) can be written using the convolution symbol “⊗” as f(x) ⊗h(x). The convolution operation is defined in the following equivalent integral equations:

$$f(x) \otimes h(x) = \int_{-\infty}^{+\infty} f(x-y)h(y)dy = \int_{-\infty}^{+\infty} f(y)h(x-y)dy \tag{2.37}$$

In Equation above, y is a dummy variable for x. In two dimensions, convolution is defined as follows

$$\begin{aligned} f(x,y) \otimes\otimes h(x,y) &= \iint_{-\infty}^{+\infty} f(x-s,y-t)h(s,t)\mathrm{d}s\mathrm{d}t \\ &= \iint_{-\infty}^{+\infty} f(s,t)h(x-s,y-t)\mathrm{d}s\mathrm{d}t \end{aligned} \tag{2.38}$$

A convolution operation on both independent variables is indicated by the symbol “⊗⊗” The notation in the expression f(x, y) ⊗ h(x, y) removes the ambiguity of the statement where f(x, y) ⊗ h(x, y), which could signify a one-dimensional convolution in terms of x, a one-dimensional convolution in terms of y, or a two-dimensional convolution

in terms of both x and y. The equation f(x, y) ⊗ h(x, y) will be used to signify a one-dimensional convolution throughout this article, and to avoid ambiguity, we will state explicitly (or make it obvious implicitly) with respect to which independent variable the convolution will be achieved. We can show (actually you should show) that the convolution operation has both commutative and associative properties so that the order and grouping of functions is completely interchangeable:

Commutative property: f(x) ⊗ g(x) = g(x) ⊗ f(x).

Associative property: f(x) ⊗ [g(x) ⊗ h(x)] = [f(x) ⊗ g(x)] ⊗ h(x).

2.2.4 Fourier transform

In one-dimension, the Fourier transform of *f(x)* is defined by the integral equation:

$$f(u) = \int_{-\infty}^{+\infty} f(x) e^{-2\pi i u x} dx, \tag{2.38}$$

where F(u) is expressed in terms of the spatial frequency variable u. Similarly, the inverse Fourier transform of F(u) gives us the function f(x) where

$$f(x) = \int_{-\infty}^{+\infty} f(u) e^{-2\pi i u x} du. \tag{2.39}$$

It's worth noting that Fourier domain functions are written in capital letters, while spatial domain functions are written in lower case, with the function letter remaining unchanged. The units of the spatial frequency variable (u) are the inverse of the units of the spatial variable (x). If x is in millimeters, then u is in fractions of millimeters. Fourier transform pairs are represented by f(x) and F(u). The following integral equations relate f(x, y) with its Fourier transform F(u, v) in two dimensions:

$$F(u, v) = \iint_{-\infty}^{+\infty} f(x, y) e^{-2\pi i (ux + vy)} dx dy \tag{2.40}$$

and

$$F(x, y) = \iint_{-\infty}^{+\infty} f(u, v) e^{-2\pi i (ux + vy)} du dv. \tag{2.41}$$

The Fourier transform contains enough fascinating properties to fill books and keep mathematicians, engineers, and physicists interested for years. Several basic definitions and properties are presented here, and as further properties are required to characterize

imaging systems, they will be introduced. The character I is occasionally used to indicate the Fourier transform to simplify the notation. We'll concentrate on a few Fourier transforms that imaging experts will find useful. The first is

$$\Im\{f[x|a]\} = aF(au) \tag{2.42}$$

and if a > 1, we see that "expansion" in the spatial domain (division of x by a) causes "contraction" in the spatial frequency domain (multiplication of u by a). Likewise, expansion in the frequency domain results in contraction in the spatial domain.

2.3 Modeling medical imaging as linear systems

The imaging process can be modeled as a system that mathematically transforms an object to a corresponding image. In a simple 2-D model, the mathematical transform (S), a function of the imaging system, determines how the object f(x, y) is transformed to the image g(x, y). For x-ray imaging, the object function f(x, y) alters the x-ray transmission at position (x, y) in the object for a thin slab of thickness dz. We will only deal with this slab for now. The image function g(x, y) is modeled as the x-ray photon fluence at (x, y) in the image (i.e., the radiographic image). The most basic form for an imaging equation is the following:

$$g(x, y) = S[f(x, y)]. \tag{2.43}$$

We'll assume linear systems for the most of our discussion on medical imaging systems. This assumption can be stated implicitly or explicitly, and while it limits us to a very limited range of attributes, it has some appealing properties. There are two fundamental features of a linear imaging system expressed in terms of a linear imaging system transform S. First, imaging the sum of two objects f_1 and f_2 yields the same result as adding the images of the items collected separately:

$$S[f_1(x, y) + f_2(x, y)] = S[f_1(x, y)] + S[f_2(x, y)] \tag{2.44}$$

This is known as the property of linear additivity. This allows us to model imaging for a thin slab under the assumption that if all slabs were modeled, we could sum the parts that compose the image. Second, if we image the object f(x, y) and then multiply the image

by a constant a, we get the same result as imaging an object of magnitude a times f(x, y). This can be represented mathematically as

$$aS[f(x,y) = S[af(x,y)] \tag{2.45}$$

where a is the multiplicative constant.

This is known as the property of linear scalar. The properties of linear additivity and scaling can be summarized in a single definition of the linear operator. The operator S is said to be linear if for every two functions f1 and f2 in its domain and for every two constants *a* and *b*, ***S*** behaves as follows:

$$aS[f_1(x,y)] + bS[f_2(x,y)] = S[a[f_1(x,y) + bf_2(x,y)] \tag{2.46}$$

An example of a linear operator is the derivative operator (d/dx). That is, if f1 and f2 are two functions, then

$$a\frac{d}{dx}[f_1(x)] + b\frac{d}{dx}[f_2(x)] = \frac{d}{dx}[af_1(x) + bf_2(x)] \tag{2.47}$$

Other examples of linear operators are the integral as well as most smoothing and edge sharpening operations. Importantly, convolution and the Fourier transform are linear operations. Investigation of how the imaging system operator *S* transforms a delta function provides insight about image formation. We begin the derivation using the two-dimensional shifting property of the delta function applied to f(x, y):

$$f(x,y) = \iint_{-\infty}^{+\infty} f(\xi,\eta)\delta(x-\xi, y-\eta)d\xi d\eta = f(x,y)\otimes\otimes\delta(x,y) \tag{2.48}$$

If the linear imaging operator S operates on the function object f(x, y) to produce a resultant image function g(x, y) such that

$$g(x,y) = S[f(x,y)] \tag{2.49}$$

Then using the linearity property of S and the integral property of a function and a shifted delta function given in Equation (2.30) , we have

$$g(x,y) = S\left[\iint_{-\infty}^{+\infty} f(\xi,\eta)\delta(x-\xi, y-\eta)d\xi d\eta\right] = \tag{2.50}$$

$$= \iint_{-\infty}^{+\infty} f(\xi,\eta) S[\delta(x-\xi, y-\eta)] d\xi d\eta$$

Note that in Equation 2.50, the term f (ξ, η) does not depend explicitly on the variables (x, y) and, therefore, is constant with respect to the operator. However, S [δ(x − ξ, y − η)] is a function of (x, y) and (ξ, η), and this new function is given the function label h (note we are using function labels in alphabetical order here from f to h):

$$S[\delta(x-\xi, y-\eta)] = h(x, y; \xi, \eta) \tag{2.51}$$

The h function can be substituted into (2.3.7) giving the following equation:

$$g(x,y) = \iint_{-\infty}^{+\infty} f(\xi,\eta) h(x, y; \xi, \eta) d\xi d\eta \tag{2.52}$$

The image value *g* is related to the object transmission *f* by the spatial response function h (Equation 2.52), which can be a function of both "object" (ξ, η) and "image" (x, y) coordinates. To model projection x-ray imaging, f(ξ, η) represents the object transmission at the point (ξ, η), while g(x, y) is the resulting image value at the point (*x*, *y*). Note: h(x, y; ξ, η) is better known to imaging physicists and engineers as the point spread function. Loosely, h(x, y; ξ, η) is the image from an infinitesimal object (i.e., delta function) at the point (ξ, η) in the object plane. In general, *h* can be a very complicated function of object and image coordinates. The importance of a linear shift-invariant system is that the point spread function *h* is the same for all locations, greatly simplifying usage. In this case, the spread in h only depends on the difference in coordinates:

$$h(x, y; \xi, \eta) = h(x-\xi, y-\eta) \tag{2.53}$$

Simply stated that if the image of a point has the same functional form as the point is moved around in the object's x-y plane (Figure 2.3a), then the imaging system is shift invariant. While this is not exactly true for projection x-ray imaging systems, it is approximately true over any sufficiently small area. Substituting Equation 2.53 into Equation 2.3.9 gives an equation for g(x, y) expressed as a convolution:

$$g(x,y) = \iint_{-\infty}^{+\infty} f(\xi,\eta) h(x-\xi, y-\eta) d\xi d\eta = f(x,y) \otimes\otimes h(x,y) \tag{2.54}$$

This result is important because it shows that an image can be expressed as the convolution of the object with the system point spread function. Equation 2.54 holds regardless of the type of imaging system, making this a very general approach to all forms of imaging systems.

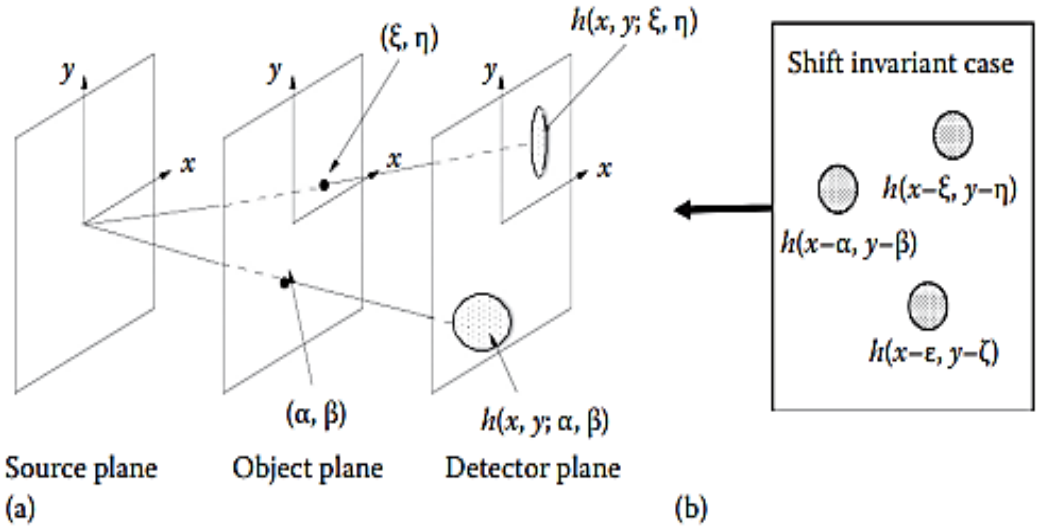

Figure 2.8 Source projection geometry. The spread function *h* changes with location in the general case (a). *h* does not change with location in a shift invariant system, but rather depends on the difference between output coordinates (b).

The image *g* can be described as "convolution" between the object *f* and the point spread function *h* in a shift invariant imaging system (Equation 2.54).

So how does this mathematical formalism apply to medical imaging (or projection x-ray imaging in particular)? We can think of an object as being comprised of an infinite number of point objects, each with differential area dξdη where the transmission at each point is equal to the object transmission f (ξ, η). We can then image a single point f (ξ, η) by fixing (ξ, η) and letting (x, y) vary, producing the point image dg(x, y) as follows:

$$dg(x,y) = f(\xi,\eta)h(x-\xi,y-\eta)d\xi d\eta \qquad (2.55)$$

Here, dg(*x*, *y*) is just an image of the point spread function *h* modulated by the object transmission at (ξ, η). Repeating by varying (ξ, η) to span the object produces a multiplicity of point spread functions, one for each point on the object that are overlaid

and added to each other. Equation 2.54 shows that the sum of all projected point spread images, obtained by integration, gives us the radiographic image g (i.e., photon fluence) produced by the transmission object *f*.

The point spread function h is the key functional component in picture creation for a linear shift invariant system. It is also used to analyze the spatial resolution of an imaging system because it monitors how object points spread away. We may determine the point spread function h(x, y) for a linear space invariant system by imaging an infinitesimal object (a delta function), and this offers a thorough measure of spatial resolution. We may use the property that the Fourier transform of the convolution of two functions equals the product of their Fourier transforms to describe the imaging process using convolution. That is, if F(u, v), G(u, v), and H(u, v) are the Fourier transforms of f(x, y), g(x, y), and h(x, y), then in the spatial frequency domain, Equation 2.54 becomes

$$G(u,v)\Im[g(x,y)] = \Im[f(x,y)\otimes\otimes h(x,y)] \tag{2.56}$$

$$G(u,v)\Im[f(x,y)]\Im[h(x,y)] = F(u,v)H(u,v) \tag{2.57}$$

$$\mathfrak{I}\{\text{Image}\} = \mathfrak{I}\{\text{Object}\}\,\mathfrak{I}\{\text{Point Spread Function}\}$$

Fourier transform changes the convolution of two functions (an integral equation) in the spatial domain into an operation multiplying two functions in the spatial-frequency domain, and simplifies many of our calculations. Fourier transforms can be searched up in standard tables or calculated in other ways, computing the product of F(u, v) and H(u, v) is typically easier than computing the convolution of f(x, y) with h(x, y). The Fourier transform of most functions requires complex multiplication for both real and imaginary portions, however in many cases this is simpler than spatial domain convolution.

2.4 Geometry based model of x-ray image formation

X-ray projection imaging is based on geometry and this concept is not obvious from the formalism presented in the previous section. In this section, we will demonstrate how projection x-ray imaging can be expressed as a convolution, while accounting for its inherent magnification. The approach (borrowed from Barrett and Swindell) will be

presented geometrically, which will help to reveal both features and limitations of projection x-ray imaging. In this derivation, we will use the geometry defined in Figure 2.9 in which the x-ray "source" is located in the x_s y_s-plane, the "object" of interest in the $x_o y_o$-plane, and the image

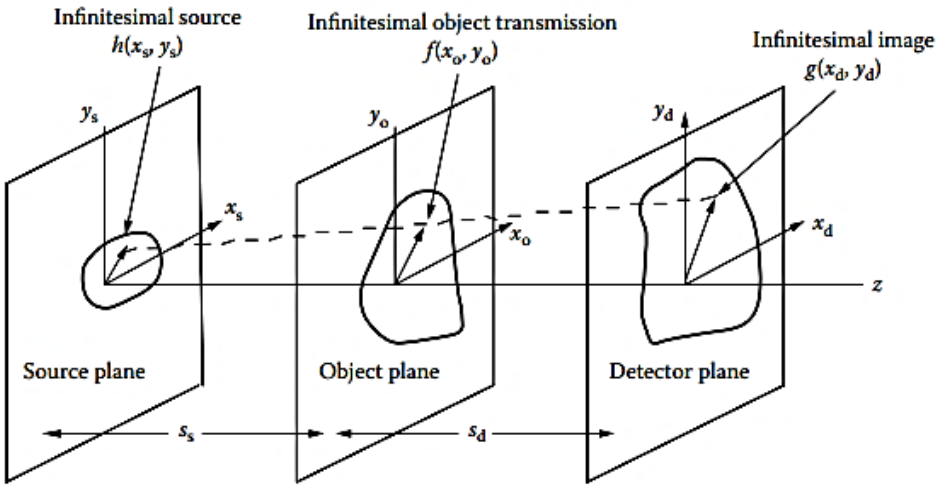

Geometry of the image formation process

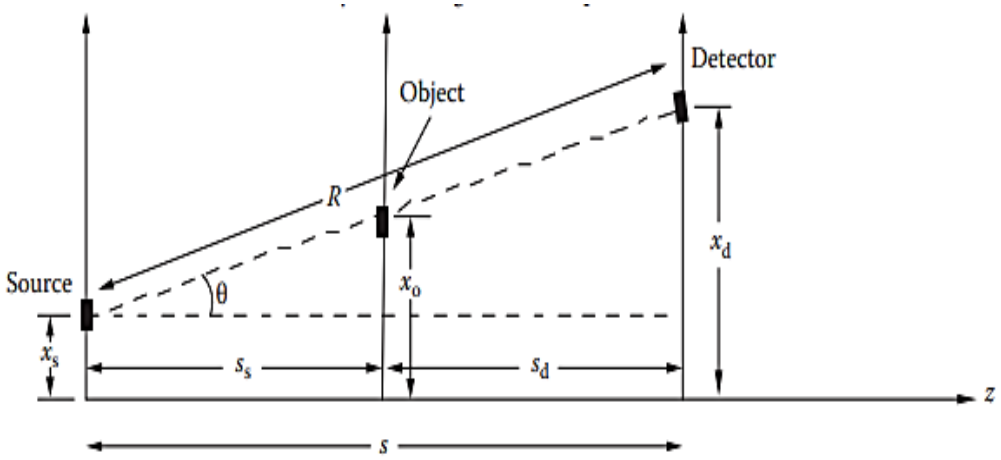

X-ray projection geometry

Figure 2.9 – Geometry and triangles used to show the relationship between variables used in the math of image formation by projection radiography. The x-ray tube focal spot is on the source plane, tissue is on the object plane, and the radiographic image is formed at the detector plane

In the "detector" $x_d y_d$-plane. The three planes are parallel and share a common z-axis. For this derivation, let us make the following assumptions: $h(x_s, y_s)$ = emitted photon

fluence (photons/area/s) at location (x_s, y_s) in the source plane. The emission is assumed to be isotropic and nonzero only where photons are emitted. f(x_o, y_o) = x-ray transmission of the object at point (x_o, y_o) in the object plane. g(x_d, y_d) = incident photon fluence in the detector plane (photons/area/s). From the definition of photon fluence g(x_d, y_d) [photons/area/s], the number of photons incident on the detector per second in a small area $dx_d dy_d$ at position x_d, y_d is

$$\frac{dN_d}{dt} = g(x_{d,}y_d)dx_d dy_d \tag{2.58}$$

The number of photons incident on the detector per second can also be calculated from the source and object geometry as

$$\frac{dN_d}{dt} = \begin{pmatrix} number\ of\ photons \\ emmited\ per\ second \end{pmatrix} \times \begin{pmatrix} Fraction\ of\ photon \\ incident\ /area\ at\ detector \end{pmatrix} \times \begin{pmatrix} transmission\ of \\ the\ object \end{pmatrix} \tag{2.59}$$

$$\frac{dN_d}{dt} = \left(\iint h(x_{s,}y_s)dx_s dy_s\right) \times \left(\frac{\cos\theta dx_d dy_d}{4\pi R^2}\right) \times \left(f(x_{\circ,}y_{\circ})\right) \tag{2.60}$$

Setting first Equation 2.58 equal to Equation 2.60, we obtain the photon fluence g incident at position $(x_{d,}y_d)$ of the detector:

$$g(x_{d,}y_d) = \iint_{-\infty}^{+\infty} \frac{\cos\theta}{4\pi R^2}\, h(x_{s,}y_s) f(x_{\circ,}y_{\circ}) dx_s dy_s \tag{2.61}$$

For simplicity, we will assume small angles where

$$\cos\theta \approx 1 \tag{2.62}$$

and

$$R \approx s = S_S + S_d \tag{2.63}$$

where s is the source-to-detector distance. Therefore, Equation 2.61 simplifies as

$$g(x_{d,}y_d) = \frac{1}{4\pi s^2} \iint_{-\infty}^{+\infty} h(x_{s,}y_s) f(x_{\circ,}y_{\circ}) dx_s dy_s \tag{2.64}$$

Equation 2.64 contains coordinates in three different planes (source, object, and detector). If there were no magnification, the detector and object coordinates would be the same, but magnification must be accounted for, so to deal with this, we will express all coordinates at the detector plane. This is important since our measurements are made at the detector plane, and magnification can be used to express corresponding coordinates at the object or source planes.

Similar triangles (Figure 2.9) that show that

$$\frac{x_\circ - x_{s,}}{s_s} = \frac{x_d - x_{\circ,}}{s_d} \tag{2.65}$$

where s_s and s_d are the distances from object to source and object to detector planes. Solving Equation 2.4.7 for $x_\circ$ leads to an equation for the x-coordinate at the object plane as a function of source and detector plane x-values:

$$x_\circ = \frac{s_d}{s_s+s_d}x_s + \frac{s_s}{s_s+s_d}x_d = \left(\frac{M-1}{M}\right)x_s + \frac{1}{M}x_d = \frac{1}{M}[(M-1)x_s + x_d] \tag{2.66}$$

Here M is the object magnification (Figure 2.10).

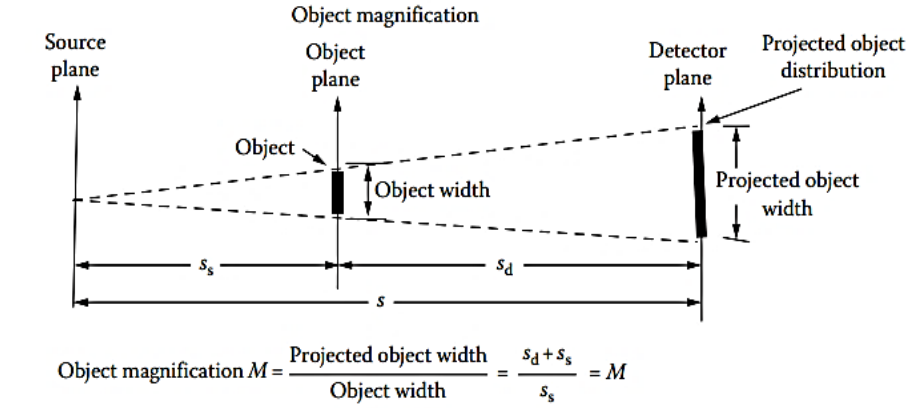

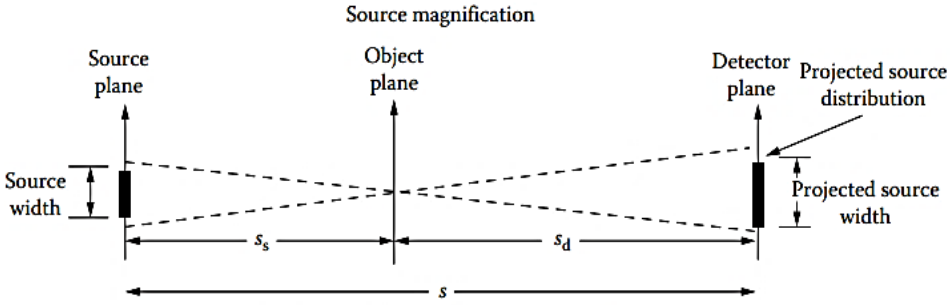

M= object magnification (defined previously)

Figure 2.10 – Geometry used to determine source and object magnification *(M)*.

The object magnification *(M)* is equal to the projected object width divided by the object width.

$$\text{Source magnification} = \frac{\text{projected source width}}{\text{Source width}} = \frac{s_d}{s_s}$$

$$M_{source} = \frac{s_d}{s_s+s_d} = \frac{s}{s_s} - 1 = M - 1$$

The source magnification ($M-1$) is equal to the projected source width (through a pinhole placed in the object plane) divided by the source width (Figure 2.9).

$$g(x_d, y_d) = \frac{1}{4\pi R^2}\frac{1}{(M\ -\ 1)^2} \times$$

$$\times \iint_{-\infty}^{+\infty} h\left(\frac{-x_s^*}{M-1}, \frac{-y_s^*}{M-1}\right) f\left(\frac{1}{M}[x_d - x_s^*], \frac{1}{M}[y_d - y_s^*]\right) dy_s^* dx_s^* \quad (2.67)$$

$$\boldsymbol{g(x,y)} = \frac{1}{(M-1)^2} h\left(\frac{-x}{M-1}, \frac{-y}{M-1}\right) \otimes\otimes f\left(\frac{x}{M}, \frac{y}{M}\right) \quad (2.68)$$

f(x, y)=object transmission

h(x, y)=source distribution

g(x, y)=photon fluence rate forming the image

M= object magnification

M-1= source magnification

Similarly, the equation for the y-coordinate is

$$y_\circ = \frac{s_d}{s_s+s_d} y_s + \frac{s_s}{s_s+s_d} y_d = \left(\frac{M-1}{M}\right) y_s + \frac{1}{M} y_d = \frac{1}{M}[(M-1)y_s + y_d] \quad (2.69)$$

Substituting x_0 and y_0 from Equations 2.68 and 2.69 into 2.66 yields

$$g(x_d, y_d) = \frac{1}{4\pi s^2} \int_{-\infty}^{+\infty} \left[\int_{-\infty}^{+\infty} h(x_s, y_s) f\left(\frac{1}{M}((M-1)x_{s,} + x_{d,}) \frac{1}{M}((M-1)y_{s,} + y_{d,})\right) dy_s\right] dx_s \quad (2.70)$$

Finally, if we project the source coordinates onto the image (detector) plane through a point in the object,

$$x_s^* = -(M-1)x \text{ and } y_s^* = -(M-1)y \quad (2.71)$$

Equation 2.4.10 can now be expressed in terms of coordinates at the detector plane based on source magnification (M − 1) and object magnification (M):

$$g(x_d, y_d) = \frac{1}{4\pi s^2}\frac{1}{(M-1)^2} \int_{-\infty}^{+\infty} \left[\int_{-\infty}^{+\infty} h\left(\frac{-x_s^*}{M-1}, \frac{-y_s^*}{M-1}\right) f\left(\frac{1}{M}[x_d - x_s^*], \frac{1}{M}[y_d - y_s^*]\right) dy_s^*\right] dx_s^* \quad (2.72)$$

On the right side of Equation 2.4.12, all coordinates indicated with "*" are in the detector plane, so the asterisk and subscripts can be dropped. This equation is then seen to be the convolution of the source distribution h with the object transmission distribution f where magnification is included:

$$g(x,y) = \frac{1}{(M-1)^2} h\left(\frac{-x}{M-1}, \frac{-y}{M-1}\right) \otimes\otimes f\left(\frac{x}{M}, \frac{y}{M}\right) \quad (2.73)$$

The subscripts were removed without loss of mathematical generality, and we have chosen the distance units of R so that 4πs2 = 1. One can calculate appropriate scale factors to account for such issues by making measurements of h with a pinhole camera. The interpretation of Equation 2.4.13 is that for projection x-ray imaging, the image "g" is formed as the convolution of the magnified source "h" with the magnified object "f". This result is consistent with the general imaging equation expressed as a convolution (Equation 2.54).

$$g(x_{d,}y_d) = \iint_{-\infty}^{+\infty} \boldsymbol{f}(\xi,\eta)\ h(x-\xi, y-\eta)d\xi d\eta = f(x,y)\otimes\otimes h(x,y)$$

This result is important because it shows that an image can be expressed as the convolution of the object with the system point spread function. Equation 2.54 holds regardless of the type of imaging system, making this a very general approach to all forms of imaging systems.

Chapter 4. Financial management, resource efficiency and resource saving

At the heart of every medical imaging technology is a sophisticated mathematical model of the measurement process and an algorithm to reconstruct an image from a measured data. Mathematics is at the core of technology. The ability to more accurately concentrate and deliver radiation to the tumor target volume has accounted for much of radiation therapy's tremendous success over the last century.

There are a lot of ways medical images in radiation therapy can be acquired. This research analyses the implications of complex mathematics in medical imaging using analytical concept of projections and reconstructions techniques in Radon transform, Fourier analysis, integral equations and sampling theory.

In modern times, the expectations with regards to scientific and engineering research are ascertain not on just the level of it discovery, which is even more complicated in terms of estimation to real life application, but rather considered on a commercial scale in the development of the sector involved. Moreover, being able to draw a commercial plan for a discovery or invention helps to search for sources of funding for the research and the commercializing the results. The aspect of commercialization seems to be more important since the commercial attractiveness of the scientific research should not be based on just exceeding technical parameters over the already existing ones, but also on how efficient the developer will be appreciated for his or her work as demanded by the market. Taking into considerations the price, customer satisfaction, project budget and many more helps to measure the worth of the research and can promote future ongoing research in the field as well. Hence, the aim of the section “Financial Management, Resource Efficiency and Resource savings” is to measure the prospects and success of a research project in order to design a mechanism for managing and acquiring special supports during the implementation stage of the project to enhance productivity.

The purpose of this section discusses the issues of competitiveness, resource efficiency and resource saving, as well as financial costs regarding the object of study of this Masters' thesis. Competitiveness analysis is carried out for this purpose. SWOT

analysis helps to identify strengths, weaknesses, opportunities and threats associated with the project, and give an idea of working with them in each particular case. The development of the project requires funds that go to the salaries of project participants and the necessary equipment, a complete list is given in the relevant section. The calculation of the resource efficiency indicator helps to make a final assessment of the technical decision on individual criteria and in general.

4.1 Potential consumers of the research results

To analyze consumers of research results, it is necessary to segment the market.

Target market – the market that includes consumers interested in the results of the research who would buy the good/service connected with the student's investigation. In this research project, the target market includes mainly cancer hospitals/clinics and research institutions.

Segmentation is the division of buyers into homogeneous groups, each of which may require a specific product (service). It is possible to apply geographic, demographic, behavioral and other criteria for segmenting the consumer market. Commercial organizations go into this type of consumers. So, it is possible to reflect the possibilities of application of this research by the most involved industries. Figure 3.1 shows the market segmentation map of services.

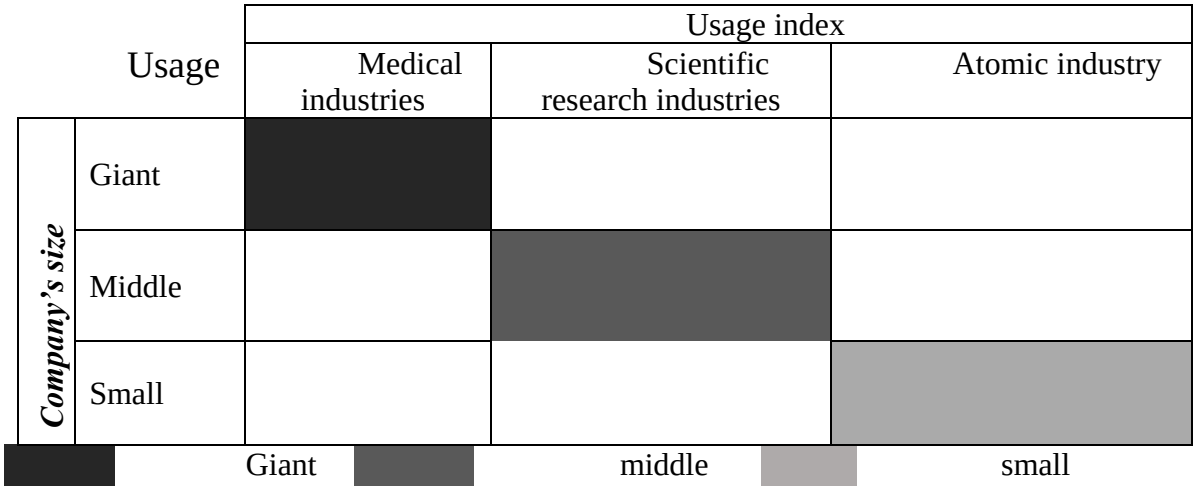

Figure 3.1. – Market segmentation map of services for the study of medical imaging

Obviously, although the research may be applied in the listed industries, it is evidently clear that medical sector takes it into more account.

4.2 Competitiveness analysis of technical solutions

In order to find sources of financing for the project, it is necessary, first, to determine the commercial value of the work. Analysis of competitive technical solutions in terms of resource efficiency and resource saving allows to evaluate the comparative effectiveness of scientific development. This analysis is advisable to carry out using an evaluation card.

First of all, it is necessary to analyze possible technical solutions and choose the best one based on the considered technical and economic criteria.

Evaluation map analysis presented in Table 4.1. The position of your research and competitors is evaluated for each indicator by you on a five-point scale, where 1 is the weakest position and 5 is the strongest. The weights of indicators determined by you in the amount should be 1. Analysis of competitive technical solutions is determined by the formula:

$$C = \sum P_i \cdot W_i, \tag{4.1}$$

where C – the competitiveness of research or a competitor;

W_i– criterion weight;

P_i – point of i-th criteria.

Table 4.1 – Evaluation card for comparison of competitive technical solutions

Evaluation criteria *example*	**Criterion weight**	**Points**		**Competitiveness** Taking into account weight coefficients	
		P_i(Matlab)	P_f(Wolfram)	C_f	C_i
1	2	3	4	7	8
Technical criteria for evaluating resource efficiency					

1. Scientific and technical potential is determined	1	3	3	0,45	0,60
2. Promising areas of commercialization of scientific and technological potential are identified	1,4	3	4	0,5	0,56
3. Author is identified, and protection of their rights is secured	2	4	4	0,8	0,9
4. Risk of treatment failure	0,1	4	4	0,64	0,7
Economic criteria for performance evaluation					
1. Competitive methods	1,4	4	4	0,4	0,5
2. Funding issues commercialization of scientific development are worked out	1,2	4	4	0,35	0,35
3. Development cost	0,7	3	4	0,54	0,6
Team for the commercialization of scientific development is formed	2	3	3	0,7	0,6
Total	**9,8**	**38**	**30**	**4,38**	**4,81**

The type of radiotherapy treatment a patient receives depends on several factors. Various processes are involved before treatment is finally delivered. These include; diagnoses, treatment simulation, image contouring treatment simulation, contouring and others. A treatment plan is dependent on the type of machine that would be used to deliver the dose.

For the competitive analysis of technical solution, two simulation techniques are considered. These are:

- MATLAB – P_i
- WOLFRAM – P_f

As discussed in previous chapters, MATLAB is very large (and growing) database of inbuilt algorithms for image processing and computer vision application. MATLAB easily allows you to test an algorithm without recompilation and also has the ability to read in a wide variety of both common. and domain-specific image formats.

WOLFRAM, on the other hand has fast development, the program can be written in a simple manner using mathematics, code compilation is slow, GUI of the Mathematica is not that good and not free to use though the cost is reasonable. In this research project, both were used but more simulation was done with MATLAB.

The results of the competitiveness analysis show that MATLAB is a better option compared to WOLFRAM.

4.3 SWOT Analysis

Complex analysis solution with the greatest competitiveness is carried out with the method of the SWOT analysis: Strengths, Weaknesses, Opportunities and Threats. Each phase in the SWOT analysis should be accurately described and follow the significance of each issue, such as:

- **Strengths:** Characteristics of the research project's competitive side. In terms of competitiveness, it demonstrates a distinct advantage or unique resource, i.e., the resources or opportunities for attaining the main goal.

- **Weaknesses**: A research project's limitations that prevent it from achieving its goals, or simply a lack of capabilities or resources in comparison to rivals.

- **Opportunities**: Occurrence of environmental circumstances that may interfere with the project, perhaps improving the project's competitive position. The analysis has several stages.

The first stage consists of describing the strengths and weaknesses of the project, identifying opportunities and threats to the project that have emerged or may appear in its external environment. The second stage consists of identifying the compatibility of the strengths and weaknesses of the project with the external environmental conditions. This compatibility or incompatibility should help to identify what strategic changes are needed.

Table 4.2 – SWOT analysis

	Strengths: 1. Able to work with acquired data from parallel x-ray beam. 2. Can reconstruct data from parallel beam projection for large industrial objects. 3. Reduction in time for the reconstruction.	**Weaknesses:** 1. Need technical know-how on MATLAB and WOLFRAM coding packages to operate at the workplace. 2. Need to understand the integral equations and their relations to each other.
Opportunities: Application in the medical field for tomographic imaging	***Strategy which based on strengths and opportunities:*** 1. It would be applicable in the medical field for tomographic imaging involving parallel beam projection techniques. 2. Distribute these codes among all industries especially nuclear related ones.	***Strategy which based on weaknesses and opportunities:*** 1. It effectiveness depends on the data acquisition stage taking by an expect in that field 2. Training of medical physicists to work with the planning program.

Threats: Lack of commercial interest in the project due to availability of more information on medical imaging	***Strategy which based on strengths and threats:*** 1. The technical knowledge on how to use the software need to be clearly explained to whoever is going to use it for reconstruction. 2. The codes should be more simplified and compact for the user.	***Strategy which based on weaknesses and threats:*** 1. Would require more research and development to keep the codes updated in order to avoid it being obsolete in the future. 2. Strong competition of alternate package from other sources.

According to the findings of this matrix's study, it can be determined that the difficulties and obstacles that this research may confront are outweighed by the research's present strengths.

4.4 Project Initiation

In the initiation processes, the initial purpose and content of the project are determined. The initial financial resources are fixed. The internal and external stakeholders of the project are determined, which will interact and influence the overall result of the research project are determined.

Project Goals and Results. Project stakeholders are persons or organizations that are actively involved in the project or whose interests may be affected both positively and negatively during the execution or as a result of the completion of the project. They can be contractors, sponsors, the public, etc. Information about the stakeholders of the project is presented in the table below.

Table 4.3 – Stakeholders of the project

Stakeholders of the project	Stakeholders of the project expectations
Cancer hospitals/clinics	Convenient in usage; High efficiency of the procedure
Research Institutions	Convenient in usage; High efficiency of the procedure
Tomsk Polytechnic University (TPU)	The acquired results could be a ground breaking finding for research in TPU.

Information about the hierarchy of project goals and criteria for achieving goals is given in the table below.

Table 4.4 – Project goals and results

Project goals	- This research analyses the implications of complex mathematics in medical imaging using analytical concept of projections and reconstructions techniques in Radon transform, Fourier analysis, integral equations and sampling theory. - To shows that an image can be expressed as the convolution of the object with the system of point spread function. - To express the modeling of medical images as linear systems
Expected results of the project	To study the physical and numerical methods and their application in medical imaging and radiotherapy using simulations.
Acceptance criteria of the project result	To study the mathematics of medical imaging in radiation therapy.

4.5 Evaluation of the project ready for commercialization

Table 4.5 – Assessment form for the degree of readiness of a scientific project for commercialization

Criteria	Degree of elaboration in the research project	Level of developers existing knowledge
The existing scientific and technical reserve is determined	4	4
Promising areas of commercialization of the scientific and technical reserve are identified	5	3
Industries and technologies (goods, services) to be offered on the market are identified	3	4
The commodity form of the scientific and technical reserve for supply at the market is defined	1	2
Authors have been identified and their rights have been protected	5	4
An assessment of the value of intellectual property was carried out	4	5
Marketing research of sales markets was carried out	3	5
A business plan for the commercialization of scientific development has been developed	2	2
The ways of promoting scientific development to the market are determined	3	5

A strategy for the implementation of scientific development has been developed	4	5
The questions of international cooperation and access to the foreign market are investigated	1	2
The ways to receive state support and benefits are analyzed	3	2
The sources of financing the commercialization of scientific development are found	2	3
The team for the commercialization of scientific development is formed	2	3
The mechanism of implementation of the scientific project has been worked out	2	3
TOTAL POINTS	44	52

4.6 Organizational Structure of the Project

The organizational structure of the project involves all participants or people who participated in the research work, the number of hours they spent and the roles they played in the research. In this research work, there were three participants. The organizational structure of the project is presented in the table below.

Table 4.6 – Project Working Group

№	**Name**	**Role in the Project**	**Functions**	**Hours spent** (working days (from table 7) × 6 hours)
1	Konstantin Brazovsky	Project Supervisor	Coordination of work activities, guidance	120

			and assistance in project implementation. Verification of results obtained.	
2	Bogdanov A.Viktorovich	Co-supervisor	Responsible for the development of the algorithms.	30
3	Asiamah Samuel Yaw	Project Executor	Work on project implementation.	700
Total:				850

4.7 Assumptions and constraints

Limitations and assumptions are summarized in table below.

Table 4.7. Limitations and assumptions

Factor	**Limitations/assumptions**
3.1. Project budget - for design	448123,78 RUB
3.1.1 Source of financing	Own funds / bank loan
3.2. Project timeline:	1 February 2022 – 25 May 2022
3.2.1 Date of approval of the project management plan	14 February 2022
3.2.2 Project completion date	25 May 2022
3. Other	Time limitations, time allocated for the research work was not enough due to lectures industrial attachment issues.

As a result of the initialization of the project, the goals and expected results were formulated, the stakeholders of the project and the financial framework were identified, which is very important for the successful completion of the project and its implementation.

4.8 Planning of Scientific and Technical Project Management

The planning process group consists of the processes that are carried out to determine the overall content of the work, clarify the goals, and develop the sequence of actions required to achieve these goals.

The scientific project management plan should include the following elements.

4.8.1 Hierarchical structure of project activities

Hierarchical Work Structure (HWS) – detailing the enlarged work structure. In the process of creating an HWS, the content of the entire project is structured and defined. It may be presented in schemes.

4.8.2 Deadlines for the project stages

As part of planning a science project, you need to build a project timeline and a Gantt Chart.

Table 4.8 – Project duration and timeline for various processes.

Job title	Duration, working days	Start date	Date of completion	Participants
Drawing up the technical assignment	15	27/01/2022	12/02/2022	Project supervisor
Literature review	20	24/02/2022	15/03/2022	Project executor
Calendar planning	3	21/03/2022	23/03/2022	Project supervisor
Research method/procedure	3	23/03/2022	25/03/2022	Project supervisor

Plan simulation	20	25/03/2022	21/04/2022	Project executor
Implementation of simulation	8	21/04/2022	29/04/2022	Co supervisor
Analysis of the results	7	30/04/2022	06/05/2022	Project supervisor
Summary of results	3	07/05/2022	9/05/2022	Project executor
Evaluation of the effectiveness of the results	3	10/05/2022	12/05/2022	Project supervisor
Drawing up a final report	10	14/05/2022	23/05/2022	Project executor
Defense Preparation	8	24/05/2022	31/05/2022	Project executor

A Gantt chart, or harmonogram, is a type of bar chart that illustrates a project schedule. This chart lists the tasks to be performed on the vertical axis, and time intervals on the horizontal axis. The width of the horizontal bars in the graph shows the duration of each activity.

Table 4.9 – Gantt chart showing the timeline of the project

№	Activities	Participants	T_c, days	Duration of the project											
				February			March			April			May		
				1	2	3	1	2	3	1	2	3	1	2	3
1	Drawing up the technical assignment	Project supervisor	**15**												
2	Literature review	Student	**20**												
3	Calendar planning	Project supervisor	**3**												
4	Research method/procedure	Project supervisor	**3**												
6	Plan simulation	Project executor	**20**												
7	Implementation of simulation	Co-supervisor	**8**												
7	Analysis of the results	Project supervisor	**7**												
8	Summary of results	Project executor	**3**												
9	Evaluation of the effectiveness of the results	Project supervisor	**3**												
10	Drawing up a final report	Project executor	**10**												
	Defense Preparation	Project executor	**8**												

Supervisor

Student

-Co supervisor

Thus, the duration of the task performed by the student and the supervisor. In general, the duration of work in calendar days for a student is 61 days, and for a supervisor and co supervisor is 31 days and 8 days respectively. The total number of working days is 100.

4.9 Scientific and Technical Research Budget

The project budget fully reflects all types of planned expenditures necessary for the implementation of the project. To find the final cost value, all calculated costs for individual items related to the manager and the student are summed. These costs include office supplies, printing costs, various equipment required for paperwork, and all costs that are associated with the purchase of special software necessary for the project.

The calculation of material costs may be also carried out according to the formula:

$$C_m = (1 + k_T) \cdot \sum_{i=1}^{m} P_i \cdot N_{consi} \quad (4.1)$$

where m – the number of types of material resources consumed in the performance of scientific research;

N_{consi} – the amount of material resources of the i-th species planned to be used when performing scientific research (units, kg, m, m^2, etc.);

P_i – the acquisition price of a unit of the i-th type of material resources consumed (rub./units, rub./kg, rub./m, rub./m^2, etc.);

k_T – coefficient taking into account transportation costs.

Prices for material resources can be set according to data posted on relevant websites on the Internet by manufacturers (or supplier organizations).

Table 4.10 shows the costs of all items.

Table 4.10 – Costs of specialized equipment and other materials

Name	Unit per measurement	Quantity (units, amount)	Price per unit (rubles)	Sum (rubles)
Stationaries	Unit	1 each	1,000	1,000
Transportation	Unit	60	50	3,000

Printing	Page	200	5	1,000
Electricity(kWh)	Unit	5	300	1500
software	Unit	1	10000	10000
Internet services	Unit	5	500	2500
Laptop	Unit	1	55000	55000
Microsoft windows 11 professional RU x 64	Unit	1	5000	5000
Kaspersky anti-virus	Unit	1	2000	2000
			Total costs for materials	
			Total transportation and purchasing costs (3-5%)	
			Total costs per article, C_m	

4.9.1 Calculation of the Depreciation

The cost of specialized equipment is recorded in the form of depreciation charges. Depreciation is a reduction in the value of an asset over time, due in particular to wear or tear. To calculate the total depreciation of the specialized equipment, the annual depreciation is calculated first, then the monthly depreciation, according the number of working days the equipment was used. The annual depreciation is calculated using the following formula:

$$N_D = \frac{1}{T} \cdot 100\%, \quad (4.2)$$

where T is the expected lifetime in years.

The life time of the laptop is approximately 10 years, the Microsoft Windows 10 license is 4 years, the anti-virus software is 1 year the wolfram software is 10 years. Then the annual depreciation rate for each of them respectively, is:

$$N_D = \frac{1}{10} \cdot 100\% = 10\ \%,$$

$$N_D = \frac{1}{4} \cdot 100\% = 25\ \%,$$

$$N_D = \frac{1}{1} \cdot 100\% = 100\ \%$$

$$N_D = \frac{1}{10} \cdot 100\% = 10\ \%$$

The daily depreciation is estimated based on the number of days the equipment is used. In this project, it is assumed that each specialized equipment is used for a period of 5 months, which is 150 days. Hence, the depreciation is calculated as such:

$$D_L = P \cdot \frac{N_D}{100} \cdot \frac{T}{365}, \quad (4.3)$$

where P is the cost of the equipment, N_D is the annual depreciation and T is the period of use in months.

$$D_L = 55000 \cdot \frac{N_D}{100} \cdot \frac{T}{365} = 55000 \cdot \frac{10}{100} \cdot \frac{150}{365} = 2260{,}27 \text{ RUB},$$

$$D_{Win10} = 5000 \cdot \frac{N_D}{100} \cdot \frac{T}{365} = 5000 \cdot \frac{25}{100} \cdot \frac{150}{365} = 513{,}7\ RUB,$$

$$D_{SS} = 2000 \cdot \frac{N_D}{100} \cdot \frac{T}{365} = 2000 \cdot \frac{100}{100} \cdot \frac{150}{365} = 821{,}92 \text{ RUB},$$

$$D_{wolfram} = 10000 \cdot \frac{N_D}{100} \cdot \frac{T}{365} = 10000 \cdot \frac{10}{100} \cdot \frac{150}{365} = 410{,}96 \text{ RUB},$$

The sum of depreciation for all equipment is:

$$D = 4006{,}85\ RUB.$$

4.9.2 Basic Salary

The basic salary includes the basic salary of scientific and engineering workers, and all other participants directly involved in the performance of this project. The amount of salary expenses is determined based on the labor intensity of the work performed and the current system of remuneration. The basic salary includes a bonus paid monthly from the salary fund (the amount is determined by the Regulations on Remuneration of Labor).

The basic salary (S_b) is calculated according to the following formula:

$$S_{\text{b}} = S_a \cdot T_{\text{w}}\,, \tag{4.4}$$

where S_b – basic salary per participant;

T_w – the duration of the work performed by the scientific and technical worker, working days;

S_a - the average daily salary of a participant, rub.

The average daily salary for a 5-day working week is calculated by the formula:

$$S_d = \frac{S_m \cdot M}{F_{\text{v}}}\,, \tag{4.5}$$

where S_m – monthly salary of a participant, rub.;

M – the number of months of work without leave during the year:

at holiday in 48 days, M = 11.2 months, 6 day per week;

F_V– valid annual fund of working time of scientific and technical personnel (251 days).

Table 4.11 – The valid annual fund of working time

Working time indicators	
Calendar number of days	365
The number of non-working days - weekend - holidays	 52 14
Loss of working time - vacation - isolation period - sick absence	 48 0
The valid annual fund of working time	251

Monthly salary is calculated by formula:

$$S_{month} = S_{base} \cdot (k_{premium} + k_{bonus}) \cdot k_{reg}, \quad (4.6)$$

where S_{base} – base salary, rubles;

$k_{premium}$ – premium rate;

k_{bonus} – bonus rate;

k_{reg} – regional rate.

Assuming, an associate professor of technical sciences, working at TPU has a salary equal to 40000 rubles, consultant (co supervisor) 30000 and a medical physicist with no experience in Tomsk has an average salary of 20000 rubles. With this in mind, the total salary of the project manager and project executor is calculated

Monthly salaries:

- For project supervisor:

$$S_{month} = S_{base} \cdot (k_{\text{premium}} + k_{bonus}) \cdot k_{reg} = 40000 \cdot (1{,}3 + 0{,}25) \cdot 1{,}3 = 80600 \text{ RUB}$$

- Co- supervisor

$$S_{month} = S_{base} \cdot (k_{\text{premium}} + k_{bonus}) \cdot k_{reg} = 30000 \cdot (1{,}3 + 0{,}25) \cdot 1{,}3 = 60450 \text{ RUB}$$

- For project executor:

$$S_{month} = S_{base} \cdot (k_{\text{premium}} + k_{bonus}) \cdot k_{reg} = 20000 \cdot (1{,}3 + 0{,}25) \cdot 1{,}3 = 40300 \text{ RUB}$$

Table 4.12 – Calculation of the base salaries

Performers	S_{base}, rubles	$k_{premium}$	k_{bonus}	k_{reg}	S_{month}, rub.	W_d, rub.	T_p, work days (from table 3.6)	W_{base}, rub.

Project supervisor	40000	1,3	0,25	1,3	80600	2686,67	31	83286,77

Continuation of the table 4.12

Project executor	20000				40300	1343,33	61	81914,30
Co-supervisor	30000				60450	2015.00	8	16120,00
Total								**181321,07**

4.9.3 Additional Salary

This point includes the amount of payments stipulated by the legislation on labor, for example, payment of regular and additional holidays; payment of time associated with state and public duties; payment for work experience, etc.

Additional salaries are calculated on the basis of 10-15% of the base salary of workers:

$$W_{add} = k_{extra} \cdot W_{base}, \quad (4.7)$$

where W_{add} – additional salary, rubles;

k_{extra} – additional salary coefficient (12%);

W_{base} – base salary, rubles.

Table 4.13 – Additional Salary

Participant	**Additional Salary, rubles**
Project supervisor	9994,33
Project executor	9829,72
Co-supervisor	1934,40
Total	21758,45

4.9.4 Social Security Pays (Labor Tax)

Social security pays/labor tax, to extra-budgetary funds are compulsory according to the norms established by the legislation of the Russian Federation to the state social insurance (SIF), pension fund (PF) and medical insurance (FCMIF) from the costs of workers. Payment to extra-budgetary funds is determined by the formula:

$$P_{social} = k_b \cdot (W_{base} + W_{add}) \quad (4.8)$$

where k_b – coefficient of deductions for labor tax.

In accordance with the Federal law of July 24, 2009 No. 212-FL, the amount of insurance contributions is set at 30%. Institutions conducting educational and scientific activities have rate - 30.2%.

Table 4.14 – Labor tax

	Project supervisor	**Co-supervisor**	**Project executor**
Coefficient of deductions	27.1 %		
Salary (basic and additional), rubles	93281,10	18054,70	91744,02
Labor tax, rubles	28170,89	5452,52	27706,69
		∑Total Tax=	**61330,10**

4.9.5 Overhead Costs

Overhead costs include other management and maintenance costs that can be allocated directly to the project. In addition, this includes expenses for the maintenance, operation and repair of equipment, production tools and equipment, buildings, structures, etc.

Overhead costs account from 30% to 90% of the amount of base and additional salary of employees.

Overhead is calculated according to the formula:

$$C_{ov} = k_{ov} \cdot (W_{base} + W_{add}) \quad (4.9)$$

where k_{ov} – overhead rate.

Table 4.15 – Overhead cost

	Project supervisor	**Co-supervisor**	**Project executor**
Overhead rate	50 %		
Salary, rubles	93281,10	18054,70	91744,02
Overhead, rubles	46640,55	9027,35	45872,01
		∑(Total Overhead) =	**101539.91**

4.9.6 Other Direct Costs

Energy costs for equipment are calculated by the formula:

$$C = P_{el} \cdot P \cdot F_{eq}, \quad (4.10)$$

where P_{el} − power rates (5.8 rubles per 1 kWh);

P − power of equipment, kW;

F_{eq} − equipment usage time, hours.

Table 4.16 – Other direct costs

	Power rates, kWh	**Power of equipment, kW**	**Equipment usage time, hr**	**Energy cost, rubles**
Laptop	5.8	0.5	427	1174,25

4.9.7 Formation of Budget Costs

The calculated cost of research is the basis for budgeting project costs.

Determining the budget for the scientific research is given in the table 3.11 below.

Table 4.17 – Items expenses grouping

Name	Cost, rubles
1. Material costs	9000,00
2. Equipment costs	72000,00
3. Basic salary	181321,07
4. Additional salary	21758,45
5. Labor tax	61330,10,
6. Overhead	101539,91
7. Other direct costs	1174,25
Total planned costs	**448123,78**

4.10 Determination of Resource (resource-saving), financial, budgetary, social and economic efficiency of research

The effectiveness of a scientific resource-saving project includes social efficiency, economic and budgetary efficiency. Public efficiency indicators take into account the socio-economic consequences of the implementation of an investment project for society as a whole, including the direct results and costs of the project, as well as costs and benefits in related sectors of the economy, environmental, social and other non-economic effects. The indicators of the economic efficiency of the project take into account the financial implications of its implementation for the enterprise implementing the project. In this case, the performance indicators of the project as a whole characterize from an economic point of view, technical, technological and organizational design solutions. Budgetary efficiency is characterized by the participation of the state in the project in terms of expenditures and revenues of budgets of all levels. In addition to the above types of efficiency, the resource effect can be distinguished (characterized by indicators reflecting the influence of innovation on the volume of production and consumption of one or

another type of resource), scientific and technical (evaluated by indicators of novelty and usefulness), etc.

4.11 Evaluation of the Absolute Effectiveness of the Project

Determination of efficiency is based on the calculation of the integral indicator of the effectiveness of scientific research. Its finding is associated with the definition of two weighted average values: financial efficiency and resource efficiency.

The integral indicator of the financial efficiency of a scientific study is obtained in the course of estimating the budget for the costs of three (or more) variants of the execution of a scientific study. For this, the largest integral indicator of the implementation of the technical problem is taken as the calculation base (as the denominator), with which the financial values for all the options are correlated.

The integral financial measure of development is defined as:

$$I_f^p = \frac{F_{p_i}}{F_{max}} \tag{4.11}$$

where I_f^p – integral financial indicator of current project;

F_{p_i} – price of i-th variant of execution;

F_{max} – the maximum cost of execution of the research project (including analogues).

In this project, $F_{p_i} = \mathbf{448123,78}$. It is assumed that, $F_{max} = \mathbf{449000,00}$.

Hence, the integral financial indicator is:

$$I_f^p = \frac{448123{,}78}{449000{,}00} = 0{,}99$$

The resulting value of the integral financial indicator of development reflects the corresponding numerical increase in the budget of development costs in times (a value greater than one), or the corresponding numerical reduction in the cost of development in times (a value less than one, but higher than zero). The integral financial indicator is equal

to 0,99. This means that, the corresponding numerical reduction in the cost of development times is 0,99.

The integral indicator of the resource efficiency of the variants of the research object can be determined as follows:

$$I_m^a = \sum_{i=1}^{n} a_i b_i^a \qquad I_m^p = \sum_{i=1}^{n} a_i b_i^p \tag{4.12}$$

where I_m – integral indicator of resource efficiency for the i-th version of the development;

a_i – the weighting factor of the i-th version of the development;

b_i^a, b_i^p – score rating of the i-th version of the development, is established by an expert on the selected rating scale;

n – number of comparison parameters.

The calculation of the integral indicator of resource efficiency is presented in the form of table 2.1.

Table 4.18 – Evaluation of the performance of the project

Criteria	**Weight criterion**	**Points**	
		I_m^p (simulation with Matlab)	I_m^a (simulation with Wolfram)
Result accuracy	0,18	5	3
Convenience in operation (user interface)	0,13	4	4
Data base	0,15	5	5
Computational speed	0,19	4	4
Test of algorithm without recompilation	0,2	5	4
Development	0,15	3	4
Total	**1**	**4,38**	**3,97**

$$I^p{}_m = \sum_{i=1}^{n} a_i b_i^a$$

$$I^p{}_m = (0{,}18 \times 5) + (0{,}13 \times 4) + (0{,}15 \times 5) + (0{,}19 \times 4) + (0{,}2 \times 5) + (0{,}15 \times 3)$$

$$I^p{}_m = 4{,}38$$

$$I^a{}_m = \sum_{i=1}^{n} a_i b_i^a$$

$$I^a{}_m = (0{,}18 \times 3) + (0{,}13 \times 4) + (0{,}15 \times 5) + (0{,}19 \times 4) + (0{,}2 \times 4) + (0{,}15 \times 4)$$

$$I^a{}_m = 3{,}97$$

The integral efficiency indicator of the scientific research project (I_{fin}^p) and of the analog (I_{fin}^a) is determined according to the formula of the integral basis of the financial integral resource efficiency:

$$I_{fin}^a = \frac{I_m^a}{I_f^a};\ I_{fin}^p = \frac{I_m^p}{I_f^p}; \tag{4.14}$$

$$I_{fin}^a = \frac{3{,}97}{1} = 3{,}97;\ I_{fin}^p = \frac{4{,}38}{0{,}99} = 4{,}42$$

Comparison of the integral indicator of the efficiency of the current project and analogs will determine the comparative efficiency the project. Comparative project efficiency:

$$E_{av} = \frac{I_{fin}^p}{I_{fin}^a} \tag{4.14}$$

Where E_{av} - is the comparative project efficiency; I_{fin}^p - integral indicator of project; I_{fin}^a - integral indicator of the analog.

$$E_{av} = \frac{4{,}42}{3{,}97} = 1{,}11$$

Thus, the effectiveness of the development is presented in table 4.19.

Table 4.19 – Efficiency of development

№	**Indicators**	**Points**	
		Project	Analog

1	Integral financial indicator	0,99	1
2	Integral resource efficiency indicator	4,38	3,97
3	Integral efficiency indicator	4,42	3,97

When project managers and executors compare the values of integral performance indicators, they can better comprehend and choose a more effective solution to the technical challenge based on financial and resource efficiency.

Chapter conclusion

In this section, stages for design and create competitive development that meet the requirements in the field of resource efficiency and resource saving were developed.

These stages include:

- development of a common economic project idea, formation of a project concept;
- organization of work on a research project;
- identification of possible research alternatives;
- research planning;
- assessing the commercial potential and prospects of scientific research from the standpoint of resource efficiency and resource saving;
- determination of resource (resource saving), financial, budget, social and economic efficiency of the project.